The Meteoritical Society

Meteoritics & Planetary Science 53, Nr 2, 167–186 (2018)
doi: 10.1111/maps.12989

Variable Tl, Pb, and Cd concentrations and isotope compositions of enstatite and ordinary chondrites—Evidence for volatile element mobilization and decay of extinct ^{205}Pb

Carl PALK[1,4], Rasmus ANDREASEN[1,5], Mark REHKÄMPER[1,*], Alison STUNT[1], Katharina KREISSIG[1], Barry COLES[1], Maria SCHÖNBÄCHLER[2], and Caroline SMITH[3]

[1]Department of Earth Science & Engineering, Imperial College London, London SW7 2AZ, UK
[2]Institute of Geochemistry and Petrology, ETH Zürich, Clausiusstrasse 25, CH-8092 Zürich, Switzerland
[3]Department of Mineralogy, Natural History Museum, London SW7 5BD, UK
[4]Present address: School of Earth Sciences, University of Bristol, Bristol BS8 1RJ, UK
[5]Present address: Department of Geoscience, Aarhus University, Høegh-Guldbergs Gade 2, 8000 Aarhus C, Denmark
*Corresponding author. E-mail: markrehk@imperial.ac.uk

(Received 01 December 2016; revision accepted 05 September 2017)

Abstract–New Tl, Pb, and Cd concentration and Tl, Pb isotope data are presented for enstatite as well as L- and LL-type ordinary chondrites, with additional Cd stable isotope results for the former. All three chondrite suites have Tl and Cd contents that vary by more than 1–2 orders of magnitude but Pb concentrations are more uniform, as a result of terrestrial Pb contamination. Model calculations based on Pb isotope compositions indicate that for more than half of the samples, more than 50% of the measured Pb contents are due to addition of modern terrestrial Pb. In part, this is responsible for the relatively young and imprecise Pb-Pb ages determined for EH, L, and LL chondrites, which are hence only of limited chronological utility. In contrast, four particularly pristine EL chondrites define a precise Pb-Pb cooling age of 4559 ± 6 Ma. The enstatite chondrites (ECs) have highly variable $\varepsilon^{114/110}$Cd of between about +3 and +70 due to stable isotope fractionation from thermal and shock metamorphism. Furthermore, nearly all enstatite meteorites display ε^{205}Tl values from −3.3 to +0.8, while a single anomalous sample is highly fractionated in both Tl and Cd isotopes. The majority of the ECs thereby define a correlation of ε^{205}Tl with $\varepsilon^{114/110}$Cd, which suggests that at least some of the Tl isotope variability reflects stable isotope fractionation rather than radiogenic ingrowth of ^{205}Tl from ^{205}Pb decay. Considering L chondrites, most ε^{205}Tl values range between −4 and +1, while two outliers with $\varepsilon^{205}\text{Tl} \leq -10$ are indicative of stable isotope fractionation. Considering only those L chondrites which are least likely to feature Pb contamination or stable Tl isotope effects, the results are in accord with the former presence of live ^{205}Pb on the parent body, with an initial $^{205}\text{Pb}/^{204}\text{Pb} = (1.5 \pm 1.4) \times 10^{-4}$, which suggests late equilibration of the Pb-Tl system 26–113 Ma after carbonaceous chondrites (CCs). The LL chondrites display highly variable ε^{205}Tl values from −12.5 to +14.9, also indicative of stable isotope effects. However, the data for three pristine LL3/LL4 chondrites display an excellent correlation between ε^{205}Tl and $^{204}\text{Pb}/^{203}$Tl. This defines an initial $^{205}\text{Pb}/^{204}\text{Pb}$ of $(1.4 \pm 0.3) \times 10^{-4}$, equivalent to a ^{205}Pb-^{205}Tl cooling age of 55 + 12/−24 Ma (31–67 Ma) after CCs.

INTRODUCTION

Extinct radionuclide systems are powerful cosmochemical tools that provide quantitative information on the presolar production sites of elements as well as the time scales of early solar system processes. The nuclide ^{205}Pb, which decays to ^{205}Tl with a half-life of 15.1 Ma (Pengra et al. 1978), has thereby

received attention for many years. This stems from the suggestion that it is unique among extinct radionuclides, as it may be produced solely by the s-process of nucleosynthesis (e.g., Blake et al. 1973; Yokoi et al. 1985; Wasserburg et al. 1994, 2006). However, it has also been posited that significant ^{205}Pb can be generated by "mini r-processing" in exploding massive stars (Heymann and Liffman 1986). Aside from its possible role as a unique nucleosynthetic tracer, the ^{205}Pb-^{205}Tl decay system has many potential uses in chronometry. Both Pb and Tl are volatile and moderately siderophile elements, so that the Pb/Tl ratios of solar system materials are affected by numerous processes, including partial evaporation and condensation, metal-silicate equilibration, and fractional crystallization of solid metal during the cooling of planetary cores. As a result, the ^{205}Pb-^{205}Tl decay system may, in principle, be useful for dating a range of early solar system processes, including volatilization during thermal processing, planetary differentiation, and core crystallization.

Astrophysical models, which predict that ^{205}Pb was sufficiently abundant in the early solar system to produce meteorite reservoirs with distinct Tl isotope compositions, prompted a number of early studies of the ^{205}Pb-^{205}Tl decay system (Anders and Stevens 1960; Ostic et al. 1969; Huey and Kohman 1972; Arden 1983; Chen and Wasserburg 1994). Definitive evidence for the former presence of live ^{205}Pb in the solar system remained elusive, however, until the investigation of Nielsen et al. (2006a). The latter study found a strong positive correlation between ε^{205}Tl and ^{204}Pb/^{203}Tl ratios for metal samples of IAB iron meteorites, and this was interpreted as an isochron from in situ decay of formerly live ^{205}Pb, following metal segregation and crystallization. While this isochron demonstrated that live ^{205}Pb was present in the solar nebula, it failed to link the ^{205}Pb-^{205}Tl decay system to an absolute time scale and hence the initial solar system abundance of ^{205}Pb remained uncertain.

Such a link, which is necessary to enable chronological application of the ^{205}Pb-^{205}Tl system, was first established by Baker et al. (2010). These workers analyzed a comprehensive suite of carbonaceous chondrites (CCs) that defined an isochron, which was interpreted to record volatile element fractionation in the solar nebula at close to 4567 Ma with an initial solar system ^{205}Pb abundance of $(^{205}\text{Pb}/^{204}\text{Pb})_{\text{SS},0} = (1.0 \pm 0.4) \times 10^{-3}$. Further evidence for radiogenic variations in Tl isotope compositions was obtained in a ^{205}Pb-^{205}Tl study of IIAB and IIIAB iron meteorites (Andreasen et al. 2012). Notably, Andreasen et al. (2012) also re-evaluated the CC isochron of Baker et al. (2010) in light of their iron meteorite results. In detail, they questioned the accuracy of the Baker et al. (2010) ^{205}Pb-^{205}Tl isochron for CCs because it included a strongly weathered desert find (NWA 801, CR2; Connolly et al. 2007) and a sample of Colony CO3 with significant Pb contamination. Following elimination of these meteorites, Andreasen et al. (2012) inferred a revised initial solar system value of $(^{205}\text{Pb}/^{204}\text{Pb})_{\text{SS},0} = 2 \pm 1 \times 10^{-3}$ and considered this result as more robust because it does not conflict with their ^{205}Pb-^{205}Tl data for IIAB irons. Given the uncertainties inherent in the ^{205}Pb-^{205}Tl isochron studies of both Baker et al. (2010) and Andreasen et al. (2012), an initial solar system ^{205}Pb abundance that combines both results to $(^{205}\text{Pb}/^{204}\text{Pb})_{\text{SS},0} = (1.8 \pm 1.2) \times 10^{-3}$ is applied here in the following.

The present study follows on from the investigations of Nielsen et al. (2006a), Baker et al. (2010), and Andreasen et al. (2012) to explore whether bulk rock samples of enstatite chondrites (ECs) and ordinary chondrites (OCs) display Tl isotope variations from the decay of ^{205}Pb, which can be exploited for chronology. Such work, however, must cope with two distinct problems that beset the application of the ^{205}Pb-^{205}Tl decay system.

First, Tl shows significant stable isotope fractionation in various terrestrial environments and meteorites (Rehkämper et al. 2002; Nielsen et al. 2006a, 2006b, 2006c, 2017; Nielsen and Rehkämper 2012). While such fractionations were initially deemed surprising due to the high atomic weight of Tl (Rehkämper and Halliday 1999), it has now been shown that stable Tl isotope effects are quite common in nature and of both mass-dependent and non–mass-dependent origin, whereby the latter are related to differences in nuclear volume and charge distribution (Schauble 2007). Such fractionations are problematic as Tl has only two stable isotopes, so there is no means to robustly differentiate between isotopic variations that are caused by radiogenic ingrowth of ^{205}Tl and stable isotope effects. Furthermore, stable isotope fractionation of Tl during nebular and parent body processes is supported by the highly mobile and volatile nature of the element (with a 50% condensation temperature of T_{C50} = 532 K; Lodders 2003), and evidence for such effects has already been found in both CCs and iron meteorites (Nielsen et al. 2006a; Baker et al. 2010). To screen their results for possible stable Tl isotope effects in CCs, Baker et al. (2010) employed stable isotope analyses of Cd. This approach to employ Cd as a monitor element is based on previous investigations, which revealed that Cd isotope compositions are readily altered by partial evaporation and condensation (Wombacher et al. 2003, 2004, 2008). The assumption that stable isotope fractionations of Cd and Tl are often at least roughly coupled is not unreasonable, given that Cd has a

condensation temperature (of T_{C50} = 652 K; Lodders 2003) similar to Tl and both elements are known to be readily volatilized and mobilized during heating and metamorphic processes (Matza and Lipschutz 1977; Ngo and Lipschutz 1980; Paul and Lipschutz 1989; Wombacher et al. 2008; Tonui et al. 2014). In addition, both Tl and Cd are thought to be concentrated in troilite during nebular condensation (Lodders 2003) and this similarity in distribution is highlighted by the excellent correlation seen in this study for the Tl and Cd concentrations of both ECs and OCs. The application of Cd stable isotopes as a monitor for Tl isotope fractionations is, furthermore, supported by the absence of radiogenic isotope effects for Cd and the availability of five major Cd isotopes (^{110}Cd to ^{114}Cd) with abundances of >10%, which enable precise and accurate stable isotope measurements with the double spike technique (Ripperger and Rehkämper 2007; Rehkämper et al. 2011). While a decoupled isotope fractionation of these two elements cannot be excluded, Cd isotope analyses presently provide the most robust means to monitor possible Tl stable isotope fractionation. Hence, such analyses were also applied here for the ECs, while previous work has already shown that Cd stable isotope fractionations appear to be fairly common for OCs, with large isotope effects (of >5‰ for ^{110}Cd/^{114}Cd) recorded in some samples (Wombacher et al. 2008).

Second, many stony and iron meteorites, including falls, are pervasively contaminated by modern terrestrial Pb (e.g., Göpel et al. 1985; Tera and Carlson 1999). Such contamination has an impact on ^{205}Pb-^{205}Tl isochron studies because they require the original uncontaminated indigenous "meteoritic" ^{204}Pb/^{203}Tl ratios, but these can be difficult, if not impossible, to recover. For some meteorites (e.g., iron meteorite metals), Pb contamination can be readily detected and quantified via Pb isotope analyses but corrections for such effects are problematic if contamination is severe and/or the indigenous meteoritic Pb isotope composition is not precisely defined. In targeted Pb isotope investigations of meteorites, the effects of terrestrial Pb contamination are commonly mitigated or avoided by extensive physical cleaning and chemical leaching of samples (Göpel et al. 1985; Amelin 2006). Such an approach was not employed here because leaching has the potential to generate significant stable isotope effects for Tl (e.g., Nielsen et al. 2013). Hence, Pb isotope measurements were carried out for all samples and these data in combination with Pb-Tl elemental ratios were employed to assess and, using model calculations, semiquantitatively determine the extent of terrestrial Pb contamination.

SAMPLES

A total of nine ECs were chosen for this study, encompassing three EH and six EL meteorites, of which five are falls (Table 1). In addition, 20 OCs were analyzed. In this case, all samples are falls, encompassing 10 L chondrites and 10 LL chondrites of petrological grades 3–6 (Table 1). While the EL6 chondrite NWA 3134 was purchased from a private collector and the EL3 chondrites MAC 02839 and PCA 91020 were obtained from the Antarctic Meteorite Collection of the NASA Johnson Space Center, all other meteorites were provided by the Natural History Museum London. The samples, obtained in the form of small chips, were initially prepared for analysis by sanding down sawn surfaces with silicon carbide paper and grinding to a powder using an alumina mortar and pestle.

ANALYTICAL METHODS

Laboratory and Reagents

The analytical work was carried out in the mass spectrometry and ISO 6 clean room laboratories of the Imperial College MAGIC Research Center. All critical sample handling was performed in ISO 4 laminar flow hoods, using Teflon PFA beakers, >18.2 MΩ cm water, and mineral acids that were purified in-house using quartz or Teflon stills. Saturated bromine water (abbreviated as Br_2-H_2O in the following) and 0.1 M HCl containing 5% dissolved SO_2 (0.1 M HCl–5% SO_2) were made up following published methods (Rehkämper and Halliday 1999). All mixtures between mineral acids and between mineral acids and Br_2-H_2O were thereby prepared on a v/v basis, while the HCl-SO_2 mixture was made up on a w/w basis. An overview of the full analytical procedure is provided in Fig. S1 in supporting information.

Sample Digestion and Aliquoting

Approximately 1.5–2 g of meteorite powder was initially digested with a mixture of 5 mL 15 M HNO_3 and 6–7 mL 28 M HF on a hotplate for several days, dried, refluxed in 5–10 mL of a 1 + 1 mixture of 15 M HNO_3 and 6 M HCl, and dried again. Following this, the samples were taken up in 5–10 mL 6 M HCl, refluxed, and then centrifuged in 15 mL PP tubes. Any residues, if present, were subjected to further acid digestion with the described procedure, but using reduced acid volumes, until perfect solutions were obtained. The final centrifuged sample solutions were then split into three aliquots (1)

Table 1. Tl, Pb, and Cd concentrations and isotope compositions of enstatite as well as L and LL ordinary chondrites.

Sample name	Class	Fall/ find	Year	Location	Shock	Tl (ng g^{-1})	2SD (ng g^{-1})	Pb (ng g^{-1})	2SD (ng g^{-1})	Cd (ng g^{-1})	2SD (ng g^{-1})
EH chondrites											
Abee	EH4	Fall	1952	Canada	S2-S4	73.2	1.5	2,497	50	857	17
Indarch	EH4	Fall	1891	Azerbaijan	S3	104	2	31,538	631	659	13
St Marks	EH5	Fall	1903	S Africa	S3	3.78	0.08	205	5	12.5	0.7
EL chondrites											
MAC 02839[a]	EL3	Find	2002	Antarctica	S3	44.5	0.9	1,653	33	286	6
PCA 91020	EL3	Find	1991	Antarctica	S5	36.7	0.7	1,234	25	486	10
Atlanta	EL6	Find	1938	USA	S2	1.60	0.03	469	9	5.65	0.70
Daniel's Kuil	EL6	Fall	1868	S Africa	S2	8.58	0.17	7,978	160	4.85	0.97
Khairpur	EL6	Fall	1873	Pakistan	S2	5.78	0.12	251	5	21.7	1.0
NWA 3134	EL6	Find	2004	Morocco		0.756	0.015	47	7	1.76	0.86
L chondrites											
Mezö-Madaras	L3.7	Fall	1852	Romania	S3	25.6	0.5	617	12	7.0	0.7
Saratov	L4	Fall	1918	Russia	S2-S3	0.45	0.01	81	2	1.8	0.2
Tennasilm	L4	Fall	1872	Estonia	S2-S3	4.84	0.10	484	10	6.6	0.7
Ausson	L5	Fall	1858	France	S3	1.55	0.03	4,850	97	4.9	0.5
Alfianello	L6	Fall	1883	Italy	S5	19.2	0.4	1,645	33		
New Concord	L6	Fall	1860	USA	S4	0.35	0.01	597	12		
Mocs 54773	L6	Fall	1882	Romania	S3	0.10	0.002	59	1	0.40	0.04
Mocs 54647	L6	Fall	1882	Romania	S3	0.11	0.002	55	1	0.40	0.04
Barwell	L6	Fall	1965	England	S3	0.15	0.003	100	2	0.52	0.05
Marion (Iowa)	L6	Fall	1847	USA		0.49	0.01	21,598	432	0.7	0.1
LL chondrites											
Bishunpur	LL3.1	Fall	1895	India	S2	19.1	0.4	1,239	25	291	29
Parnallee	LL3.6	Fall	1857	India	S3	0.56	0.01	265	5	1.4	0.1
Benares	LL4	Fall	1798	India		0.57	0.01	1,899	38	1.4	0.1
Soko-Banja	LL4	Fall	1877	Serbia		1.28	0.03	564	11	3.6	0.4
Khanpur	LL5	Fall	1932	India		1.50	0.03	656	13	16	2
Olivenza	LL5	Fall	1924	Spain	S3	16.0	0.3	486	10	40	4
Tuxtuac	LL5	Fall	1975	Mexico	S2	18.5	0.4	267	5	6.9	0.7
Appley Bridge	LL6	Fall	1914	England	S3	0.38	0.01	714	14	0.84	0.08
Dhurmsala	LL6	Fall	1860	India	S3	0.34	0.01	694	14	11	1
Mangwendi	LL6	Fall	1934	Zimbabwe		10.8	0.2	503	10	3.1	0.3
Terrestrial											
AGV-2				USGS						67.7	2.3
AGV-2—literature values				USGS						66.6[b]	

Shock stages from Bennett and McSween (1996), Friedrich et al. (2004), Gattacceca et al. (2005), Izawa et al. (2011), Rubin (1994, 2004), Rubin et al. (1997), and Stöffler et al. (1991). The uncertainties for the concentration data are ±2% for Tl and Pb, ±2% for Cd in ECs, and ±10% for Cd in OCs. The quoted uncertainties for the isotopic data were determined as follows: for ε^{205}Tl based on 2SD of multiple bracketing standard runs; for $\varepsilon^{114/110}$Cd based on internal 2SE precision of sample runs (typically similar to 2SD of multiple standard runs), using a minimum value of 0.5; for Pb isotopes based on 2SE precision of samples and/or bracketing standard runs. The calculated $f_{met\text{-}Pb}$ values denote the molar fraction of indigenous meteoritic Pb present in the analyzed samples (see supporting information).
[a]MAC 02839 and MAC 02837 are paired (Righter and Satterwhite 2004). [b]Wiggenhauser et al. (2016). [c]Baker et al. (2009). [d]Prytulak et al. (2013). [e]Hettmann et al. (2014). [f]Selected "best" values from GeoReM database (Jochum et al. 2005).

a split of ~2.5% was used for Tl and Pb concentration measurements by isotope dilution (ID); (2) a similarly small aliquot was taken for an initial determination of Cd concentrations by ID; (3) the majority of the solutions were reserved for the determination of Tl, Pb, and (for the ECs) Cd isotope compositions (see Fig. S1).

Processing of Samples Prior to Mass Spectrometry

Samples for ID Concentration Measurements of Tl, Pb, and Cd

Highly enriched tracer solutions of ^{203}Tl and ^{208}Pb were added to and equilibrated with the Tl-Pb ID sample aliquots. The solutions were then dried,

$^{204}Pb/^{203}Tl$	2SD	$\varepsilon^{205}Tl$	2SD	$\varepsilon^{114/110}$ Cd	2SD	$^{206}Pb/^{204}Pb$	2SE	$^{207}Pb/^{204}Pb$	2SE	$^{208}Pb/^{204}Pb$	2SE	$f_{met\text{-}Pb}$
2.16	0.01	−3.3	1.0	2.9	0.5	10.336	0.002	10.972	0.001	30.481	0.003	0.83–0.87
13.9	0.1	−2.7	0.5	4.2	0.5	18.137	0.001	15.143	0.001	38.076	0.004	≤0.10
2.63	0.07	0.8	0.5	9.7	1.0	16.625	0.001	14.794	0.001	36.424	0.004	0.27–0.53
2.44	0.01	−1.3	0.5	7.6	0.6	9.584	0.001	10.480	0.001	29.765	0.004	≥0.98
2.21	0.01	22.2	0.5	72.9	0.6	9.609	0.001	10.496	0.001	29.842	0.004	≥0.98
13.6	0.1	−1.8	0.5	10.4	1.3	17.868	0.001	15.320	0.001	38.028	0.003	≤0.19
42.4	0.1											
2.67	0.04	−1.0	0.5	65.7	0.9	10.976	0.002	11.339	0.001	31.364	0.004	0.88–0.99
1.88	0.26	−1.4	0.5	6.9	2.1	28.085	0.002	21.977	0.002	52.917	0.004	(0.32–0.89)
1.48	0.21	−1.0	0.3			11.292	0.002	11.518	0.002	31.313	0.004	(0.76–0.88)
6.7	0.9	1.0	0.8			25.530	0.002	20.426	0.002	44.199	0.004	0.38–0.91
5.3	0.7	−21.3	0.5			14.616	0.002	13.555	0.002	34.643	0.004	0.35–0.58
144	20	−4.2	0.5			18.415	0.002	15.703	0.002	38.456	0.004	≤0.07
4.1	0.6	−2.1	0.5			17.15	0.01	15.72	0.01	36.97	0.01	(0.05–0.33)
76.3	10.7	−9.9	0.9			19.60	0.01	16.42	0.01	39.67	0.01	(≤0.14)
15.6	2.2					41.616	0.002	30.012	0.002	58.962	0.004	(0.68–0.74)
13.7	1.9	0.3	5.9			39.190	0.002	28.432	0.002	59.271	0.004	(0.43–0.92)
24.8	3.5	−3.9	1.1			26.449	0.002	21.223	0.002	45.830	0.004	0.20–0.40
2,030	284	−2.6	0.6			18.379	0.002	15.640	0.002	38.405	0.004	≤0.07
3.3	0.5	−7.5	0.5			15.435	0.002	13.996	0.002	35.458	0.004	(0.18–0.37)
28.1	3.9	7.1	1.6			11.85	0.01	11.93	0.01	31.95	0.01	≥0.82
152	21	−2.7	1.7			18.21	0.01	15.76	0.01	38.77	0.01	(≤0.11)
24.9	3.5	2.7	0.5			13.057	0.002	12.608	0.002	33.108	0.004	0.53–0.72
20.0	2.8	−6.0	0.6			18.752	0.002	16.375	0.002	38.223	0.004	(≤0.17)
1.71	0.24	14.9	0.4			13.17	0.01	12.62	0.01	33.18	0.01	0.53–0.71
0.66	0.09	−12.5	0.3			18.089	0.002	15.465	0.002	38.870	0.004	0.10–0.46
90.2	12.6	0.1	2.8			17.37	0.01	15.25	0.01	37.21	0.01	(≤0.27)
90.1	12.6	−10.9	0.6			19.411	0.002	16.344	0.002	39.317	0.004	(≤0.13)
2.35	0.33	−1.4	0.4			15.87	0.01	14.58	0.01	35.80	0.01	(0.19–0.43)
		−2.4	0.5	1.5	0.8	18.867	0.001	15.622	0.001	38.551	0.005	
		−1.9[c]	0.5	1.1[b]	1.1	18.864-		15.609-		38.501-		
		−2.7[d]	0.4			18.874	[f]	15.621	[f]	38.552	[f]	
		−3.0[e]	0.6									

redissolved in 1 mL 0.2 M HBr containing 1% of Br_2-H_2O (0.2 M HBr – 1% Br_2-H_2O hereafter), and Tl and Pb were separated with the same ion exchange procedure that was used by Baker et al. (2009) for their ID aliquots (see Table S1 in supporting information).

The Cd ID sample aliquots were spiked with a ^{113}Cd-^{111}Cd double spike (Xue et al. 2012), evaporated to dryness, and taken up again in ~500 µL 3 M HCl. The ion exchange procedure that was then applied for the separation of Cd was modified from the methodology of Wombacher et al. (2003) (see Table S2 in supporting information).

Samples for Determination of Tl, Pb, and Cd Isotope Compositions

The employed chromatographic methods were modified from Baker et al. (2010) and enable the separation and purification of separate Tl, Pb, and Cd fractions from a single solution aliquot prior to isotopic analysis. To this end, an appropriate weight of ^{113}Cd-^{111}Cd double spike was first added to the major sample aliquots from the initial digestion. Following equilibration by refluxing, the solutions were dried and the residues were taken up in 1 M HCl–2% Br_2-H_2O, ready for the first stage of the purification procedure. In this first step, a combined Pb-Cd and a separate Tl fraction were isolated from the sample matrix, using a procedure modified from the initial chemistry protocol employed by Baker et al. (2010) (see Fig. S1; Table S3 in supporting information). Importantly, this new method achieves nearly quantitative yields for all three elements on a routine basis.

A further small resin column was thereafter employed for the purification of the Tl fractions, following methods modified from Rehkämper and Halliday (1999) (see Table S4 in supporting information). The combined Pb-Cd fractions were dried and processed through a second stage of anion exchange chromatography to separate Pb and Cd from each other and remaining matrix elements (see Table S5 of the supporting information). The Pb fractions obtained in this second stage of the purification procedure were already sufficiently clean for isotopic analysis, while additional cleanup steps were necessary for Cd. In detail, Cd purification was achieved in two stages using small resin columns following procedures modified from Wombacher et al. (2003). An initial Cd separation by anion exchange chromatography was thereby followed by a cleanup column with TRU resin to better isolate Cd from potentially problematic elements, such as Sn and Mo (see Table S6 in supporting information).

Mass Spectrometry

All isotopic measurements were carried out with a Nu Instruments Nu Plasma HR MC-ICP-MS, using either an Aridus, Aridus II, or a Nu Instruments DSN desolvating sample introduction system fitted with glass or PFA nebulizers that were operated at a flow rate of about 100–130 μL min^{-1}. Prior to the analyses, the purified elemental fractions were dissolved in an appropriate volume of either 0.1 M HNO_3 (for Pb and Cd) or 0.1 M HNO_3–0.1% H_2SO_4 (v/v; for Tl).

Isotope Dilution Concentration Measurements for Tl, Pb, and Cd

The purified Tl ID fractions were doped with NIST SRM 981 Pb and an in-house Pt standard solution, and both ^{208}Pb/^{206}Pb and ^{198}Pt/^{196}Pt were monitored during the ^{203}Tl/^{205}Tl ID measurements for correction of the instrumental mass bias. While the mass bias correction of the Tl data using Pb provides more precise results (due to the highly correlated mass bias behavior of both elements), the less precise Pt-normalized Tl isotope data are superior for samples that contain small residual amounts of sample-derived Pb. Such sample-derived Pb produces systematic errors in the mass bias correction and may be present in the Tl ID samples, as the Tl is not purified by a second step of column chemistry (Table S2) (Nielsen et al. 2004). The Pb ID fractions were doped with NIST SRM 997 Tl, allowing use of the ^{205}Tl/^{203}Tl ratios for the correction of the instrumental mass bias encountered by ^{208}Pb/^{206}Pb. For Cd, the ^{111}Cd/^{110}Cd ratios were employed for the ID concentration calculations to avoid isotopes that suffer from isobaric interferences of Sn, which was present in traces in the Cd ID fractions.

Isotope Composition Measurements for Tl, Pb, and Cd

The determination of Tl isotope compositions largely followed the procedures of Baker et al. (2009). The purified Tl fractions were thereby doped with NIST SRM 981 Pb and a combination of external normalization to ^{208}Pb/^{206}Pb and standard-sample bracketing was applied for mass bias correction. All results are reported in ε notation, whereby

$$\varepsilon^{205}\mathrm{Tl} = \left(\frac{\left(^{205}\mathrm{Tl}/^{203}\mathrm{Tl}\right)_{\mathrm{sample}}}{\left(^{205}\mathrm{Tl}/^{203}\mathrm{Tl}\right)_{\mathrm{std}}} - 1\right) \times 10,000. \qquad (1)$$

A solution of NIST SRM 997 Tl was used as $\varepsilon^{205}\mathrm{Tl} = 0$ standard throughout. Multiple analyses of the Aldrich Tl secondary reference material yielded a mean of $\varepsilon^{205}\mathrm{Tl} = -1.15 \pm 0.42$ (2SD, $n = 3$), in accord with the published average of -0.81 ± 0.33 (2SD, $n = 133$; Nielsen and Rehkämper 2012).

The Pb isotope measurements were conducted using standard-sample bracketing and external normalization relative to the ^{205}Tl/^{203}Tl ratio of admixed NIST SRM 997 Tl for mass bias correction. The analytical methods were similar to those outlined in Rehkämper and Mezger (2000), and all results are reported relative to the NIST SRM 981 Pb data of Galer and Abouchami (1998).

The stable Cd isotope measurements utilized previously described data acquisition and reduction methods (Ripperger and Rehkämper 2007; Xue et al. 2012). The Cd isotope data collected during the mass spectrometric analyses of the sample–double spike mixtures—were processed to determine the "true" isotope compositions of the unspiked samples, which were

corrected for both instrumental mass bias and isobaric interferences. All results are reported in $\varepsilon^{114/110}$Cd notation, calculated analogous to Equation 1 using the ^{114}Cd/^{110}Cd isotope ratio. The $\varepsilon^{114/110}$Cd data are thereby given relative to NIST SRM 3108 Cd (Abouchami et al. 2013).

Blanks and Geological Reference Materials

Full procedural blanks were processed through the digestion and chemical separation procedure with every batch of 6–12 samples. For Tl and Cd, the mean blanks were about 5 and 50 pg, respectively (all blanks given are for a 100% sample aliquot). For samples with the lowest Tl and Cd contents of about 0.1 and 0.5 ng g^{-1}, respectively (Table 1), this amounts to blank contributions to the total element contents of about 3% for Tl and 5% for Cd. The great majority of the samples, however, are more enriched in these elements and the blank contributions are therefore mostly <1%. Given these observations, the Tl and Cd concentrations were corrected for blank contributions, while no corrections were undertaken for the isotope compositions, because such corrections are smaller than the analytical uncertainty for most samples and are poorly constrained for all (as the isotope composition of the blank was not determined).

The total procedural Pb blanks were significantly higher at between 0.9 and 2.8 ng. These relatively high blanks are attributed to the use of modified household hotplates for initial sample digestions, while dedicated Teflon-coated hotplates were employed in subsequent sample preparation steps. The latter conclusion follows from tests with the USGS AGV-2 reference material; when this sample was processed using only Teflon-coated hotplates, the corresponding Pb blanks averaged ~90 pg. Despite the relatively high Pb blanks, the blank contribution to the total Pb content of samples is only moderate to negligible. For the samples with the lowest Pb concentrations (~50 ng g^{-1}; Table 1), the blank contributes <3% to the total Pb budgets, but 20 of 26 samples have Pb concentration exceeding 200 ng g^{-1}, where the blank additions amount to <1%. Consequently, the measured Pb concentrations were blank-corrected but no corrections were applied to the isotope compositions, as such corrections would be minor and highly uncertain, given the uncertainty of the blank isotope composition.

Analyses of the USGS geological reference material AGV-2 yielded Tl, Pb, and Cd isotope compositions and Cd concentrations in good agreement with recently published results, thereby demonstrating the robustness of our methods (Table 1).

RESULTS AND DISCUSSION

Tl, Pb, and Cd Concentrations

Enstatite Chondrites

The Tl concentrations of the ECs vary by more than 2 orders of magnitude, from less than 1 ng g^{-1} to more than 100 ng g^{-1} (Fig. 1, Table 1). The Cd contents of these meteorites are similarly variable with concentrations from about 1.8 ng g^{-1} to nearly 860 ng g^{-1}. Clear systematics are apparent for both elements. First, the analyzed EH and the EL chondrites display similar abundance variations for both elements. Second, the less metamorphosed group of each clan (EH4 and EL3) generally has higher Tl, Cd concentrations compared to the more strongly metamorphosed meteorites (EH5 and EL6).

Comparable systematics are seen for Pb (Fig. 1, Table 1). For this element, the concentrations in ECs range from <50 ng g^{-1} to more than 31,000 ng g^{-1}, with the less metamorphosed EH4/EL3 samples generally displaying higher Pb contents than the more equilibrated samples of groups EH5 and EL6. However, the EL6 Daniel's Kuil has a higher Pb content (of ~8000 ng g^{-1}) than the two analyzed EL3s (with <1700 ng g^{-1} Pb), while the EH4 Indarch has an unusually high Pb abundance of more than 31,000 ng g^{-1}. These latter observations most likely reflect significant contamination of both samples with terrestrial Pb and such contamination is expected to be more severe for Pb than for Tl, Cd, and other elements due to the ubiquity of anthropogenic Pb in the environment.

Notably, the combined EC data set reveals rather well-correlated Cd and Tl concentrations (R^2 = 0.83; Fig. 1a) with a mean Cd/Tl ratio of about 6. The plots of Pb abundance versus Tl and Cd (Figs. 1b and 1c) furthermore reveal that all but three of the samples are in accord with strongly correlated behavior between these elements. The same three samples, Indarch, Daniel's Kuil, and Atlanta, are thereby offset from both correlations (Figs. 1b and 1c) most likely due to recent terrestrial Pb contamination. The remaining meteorites display correlations with R^2 values of 0.99 and 0.88 for the Pb versus Tl and Cd trends, respectively, highlighting that all three elements may be controlled by similar processes and/or concentrated in the same phases in these meteorites.

L Chondrites

The Tl and Cd concentrations of the L chondrites vary by more than an order of magnitude, from about 0.1 to 26 ng g^{-1} and 0.4 to 7 ng g^{-1}, respectively (Fig. 1; Table 1). For both elements, the less

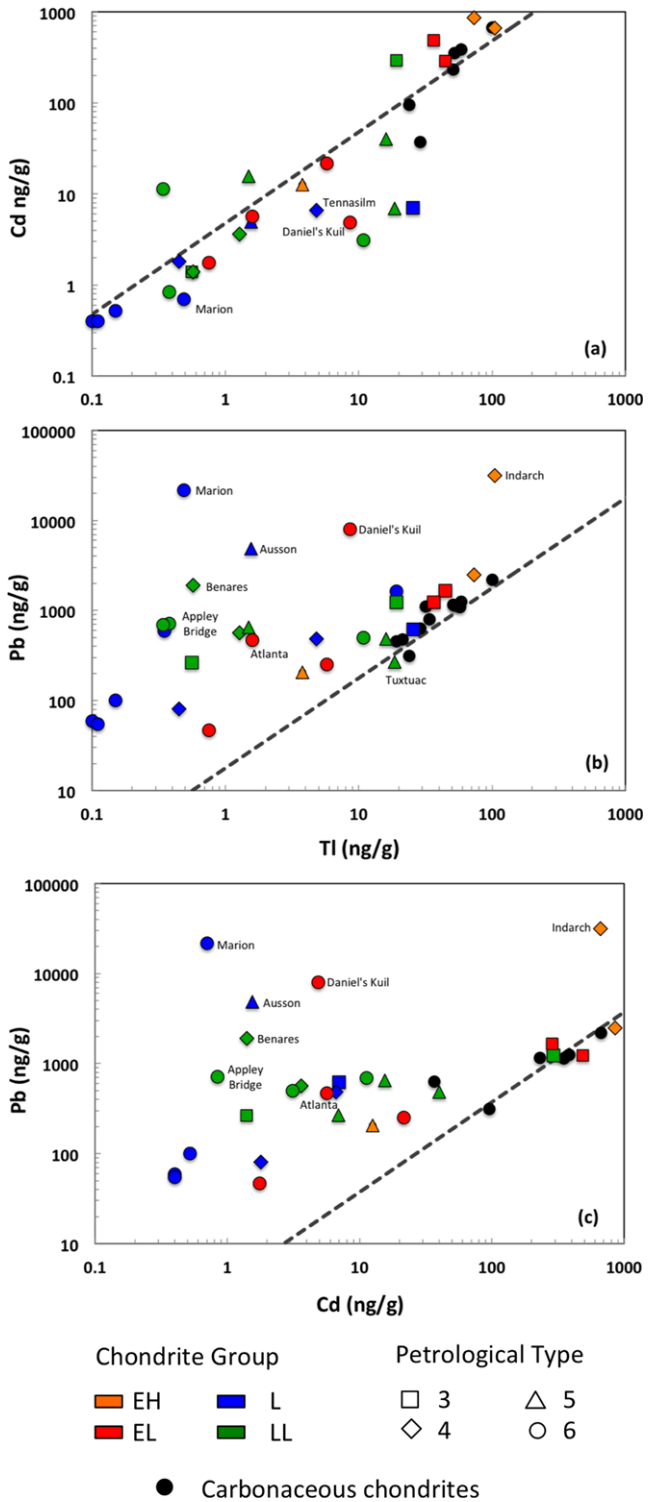

Fig. 1. Plots of (a) Cd versus Tl, (b) Pb versus Tl, and (c) Pb versus Cd concentrations for EH and EL enstatite chondrites as well as L- and LL-type ordinary chondrites. Data for carbonaceous chondrites are shown for comparison (Baker et al. 2010). The hashed lines denote the CI chondritic reference lines defined by Cd/Tl = 4.755, Pb/Tl = 17.69, and Pb/Cd = 3.721 (Palme and Jones 2005). Selected samples specifically mentioned in the text are labeled in the panels. (Color figure can be viewed at wileyonlinelibrary.com.)

metamorphosed samples (of type L3/L4) tend to have higher concentrations than the more equilibrated L5/L6 chondrites. The Pb concentrations of the L chondrites are also highly variable at between 55 and 21,000 ng g^{-1} (Fig. 1; Table 1) and there is no obvious correlation with petrographic type. Rather, it is apparent that Pb abundances are particularly variable for meteorites with relatively low Tl and Cd contents. Most likely, this reflects that samples with low indigenous volatile contents (as shown by Tl, Cd) are most susceptible to contamination by modern terrestrial Pb (Figs. 1b and 1c). Given these elemental systematics, it is unsurprising that Cd and Tl display somewhat correlated behavior in L chondrites, while there is no clear correlation of Pb with either Tl or Cd.

LL Chondrites

The Tl and Cd concentrations of LL chondrites vary by roughly 2 orders of magnitude, from about 0.3 to 19 ng g^{-1} and 0.8 to 290 ng g^{-1}, respectively (Fig. 1; Table 1). In contrast to ECs and L chondrites, the correlation between Tl and Cd abundances is less well developed and there is no systematic variation of the concentrations with petrographic grade. In comparison, the Pb contents vary by less than a factor of 10, between about 270 and 1900 ng g^{-1} and no correlation is apparent between Pb and Tl or Cd concentrations (Figs. 1b and 1c). Rather, Pb abundances are fairly variable at both high and low Tl and Cd contents, most likely due to alteration of the pristine "meteoritic" Pb budgets by terrestrial alteration and contamination.

Overall Concentration Trends

Overall, the ECs and OCs display much more variable Pb, Tl, and Cd contents than the CCs of groups CI, CM, CO, CR, and CV that were analyzed by Baker et al. (2010) (Fig. 1). Baker et al. (2010) did not publish Cd concentrations for the CCs but results for six of their samples are now provided here (see Appendix). In detail, the EC and particularly the OC samples extend to significantly lower Pb, Tl, and Cd contents than the CCs, reflecting more severe volatile element depletion. In the following, the trends of the data are compared with the CI chondritic reference lines, defined by Cd/Tl = 4.76, Pb/Tl = 17.7, and Pb/Cd = 3.72 (Palme and Jones 2005), which are also shown in Fig. 1.

In a plot of Cd versus Tl contents, the EC, OC (and CC) data fall on a generally well-defined trend that essentially overlaps with the CI reference line (Fig. 1a). This suggests that the cosmochemical behavior of Cd and Tl is highly correlated during the volatile depletion processes that occurred in both the solar nebula and on meteorite parent bodies. However, a significant number

of meteorites plot below the CI reference line at intermediate Tl contents of about 4–40 ng g^{-1} (Fig. 1a). Possibly, this may reflect preferential loss of Cd relative to Tl either during nebular processing or volatile remobilization. The lower condensation temperature of Tl in comparison to Cd (532 K versus 652 K; Lodders 2003) thereby argues against the former interpretation, while the latter is supported by the higher metamorphic mobility of Cd (relative to Tl), which has been inferred in previous work (e.g., Matza and Lipschutz 1977; Ngo and Lipschutz 1980; Paul and Lipschutz 1989; Tonui et al. 2014).

In the diagrams of Pb versus Tl and Cd, many EC and most OC samples plot above and to the left of the CI reference lines (Figs. 1b and 1c). These systematics most likely result from a combination of two processes. First, Pb appears to be less impacted than Tl and Cd by the depletion processes that reduced the volatile element abundances of ECs and OCs relative to CIs. This may be due to the higher condensation temperature of Pb (T_{C50} = 727 K; Lodders 2003) or because it resides in more resistant phases (Fe alloys) than Tl and Cd, which are primarily hosted by troilite following nebular condensation (Lodders 2003). Second, given that the samples were not chemically leached prior to dissolution, it is likely that many of the meteorites are contaminated with substantial quantities of terrestrial Pb.

Pb Isotope Compositions and Evaluation of Terrestrial Pb Contamination

In the following, the measured Pb isotope compositions are employed to assess the extent to which the analyzed samples were affected by the addition of terrestrial Pb (Fig. 2). A plot of $^{207}Pb/^{204}Pb$ versus $^{206}Pb/^{204}Pb$ for all ECs and OCs (Fig. 2a) demonstrates that the Pb isotope data fall into three broad groups. (1) Samples with $^{206}Pb/^{204}Pb \leq 13.5$ have near-primordial indigenous meteoritic Pb, similar to that seen in many CCs (e.g., Baker et al. 2010). This group encompasses four ECs, a single L chondrite, and three LL meteorites. (2) Four L chondrites and NWA 3134 EL6 have radiogenic Pb isotope compositions with $^{206}Pb/^{204}Pb \geq 25$. This radiogenic Pb is most likely also of indigenous origin, reflecting in situ decay of U and Th at high μ ($^{238}U/^{204}Pb$) and variable κ ($^{232}Th/^{204}Pb$) values (e.g., Manhes and Allègre 1978; Unruh 1982; Göpel et al. 1994). (3) The largest group of samples, however, has intermediate Pb isotope ratios with $^{206}Pb/^{204}Pb$ of between 14.5 and 19.5. While such isotope compositions could reflect indigenous meteoritic Pb that was produced in meteorites with intermediate μ, there are several lines of evidence, which demonstrate

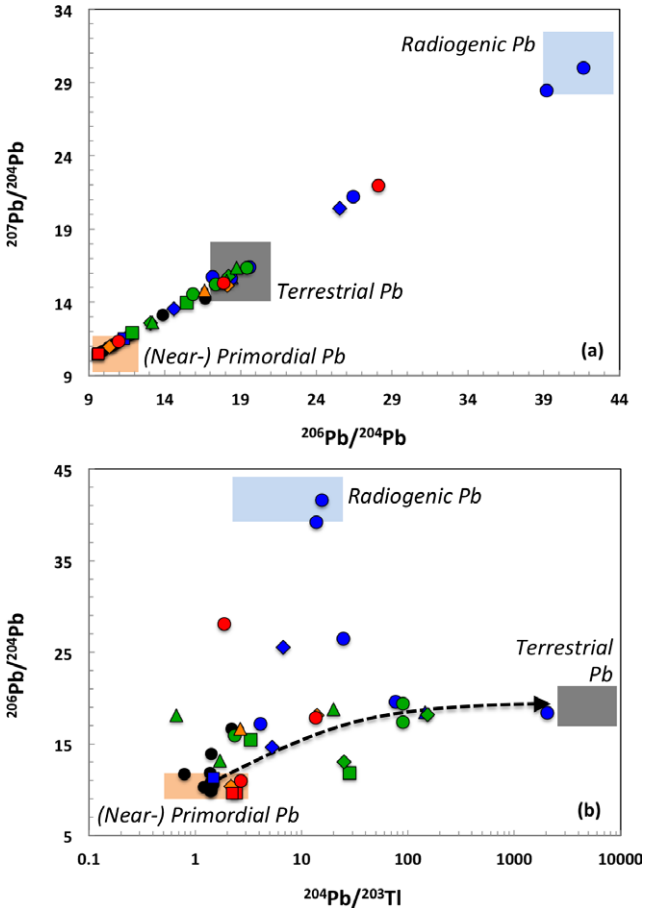

Fig. 2. Plots of (a) $^{207}Pb/^{204}Pb$ versus $^{206}Pb/^{204}Pb$ and (b) $^{206}Pb/^{204}Pb$ versus $^{204}Pb/^{203}Tl$ (in logarithmic scale) for the enstatite and ordinary chondrites analyzed here. Data for carbonaceous chondrites are shown for comparison (Baker et al. 2010). The boxes approximate the compositions of the three Pb endmembers of (1) "near-primordial" indigenous meteoritic Pb; (2) "radiogenic Pb" also inferred to be of indigenous origin; and (3) "terrestrial Pb," added as contamination (see text for details). The hashed line in (b) denotes the mixing trend generated by contamination of near-primordial Pb ($^{204}Pb/^{203}Tl$ = 1.5; $^{206}Pb/^{204}Pb$ = 10) with terrestrial Pb ($^{204}Pb/^{203}Tl$ = 1000; $^{206}Pb/^{204}Pb$ = 19). Symbols are as defined in the legend of Fig. 1. (Color figure can be viewed at wileyonlinelibrary.com.)

that the majority of samples from this group are pervasively contaminated with modern terrestrial Pb, characterized by $^{206}Pb/^{204}Pb$ of about 16.0–19.5 (Göpel et al. 1985). In particular, many samples with such silicate Earth-like Pb isotopes also feature elevated Pb concentrations (Fig. 1). This includes, for example, the ECs Indarch and Atlanta; the L5/L6 chondrites Ausson, New Concord, and Marion (Iowa); as well as the LL4/LL5/LL6 meteorites Benares, Khanpur, Appley Bridge, and Dhurmsala.

A $^{206}Pb/^{204}Pb$ versus $^{204}Pb/^{203}Tl$ diagram is also useful for distinguishing between the three components of

Pb present in the samples—primordial Pb, radiogenic Pb from in situ U, Th decay (which together comprise the indigenous meteoritic Pb of the meteorites), and extraneous terrestrial Pb from contamination of the meteorites (Fig. 2b). The plot thereby reveals two separate trends of data emanating from (near-) primordial meteoritic Pb characterized by $^{206}Pb/^{204}Pb$ ratios of between 9.5 and 10.5. (1) A very steep trend toward a composition characterized by $^{206}Pb/^{204}Pb > 40$ and $^{204}Pb/^{203}Tl$ of between about 2 and 20. This is defined by samples with low Pb contents of ≤100 ng g^{-1} and hence reflects ingrowth of radiogenic Pb formed at high μ, in accord with the results of previous studies (e.g., Manhes and Allègre 1978; Unruh 1982; Göpel et al. 1994). (2) A shallower, curved trend toward $^{206}Pb/^{204}Pb \approx 18$ and high $^{204}Pb/^{203}Tl$ values of >100 reflects the addition of terrestrial Pb. Combining the information from Pb concentrations (Fig. 1) and isotope compositions (Fig. 2) hence suggests that many, if not most, samples with $^{204}Pb/^{203}Tl$ ratios larger than about 10–20 are probably significantly affected by terrestrial Pb contamination, and this questions their use in isochron diagrams that attempt to exploit the extinct ^{205}Pb-^{205}Tl decay system for chronology. Assessments of data quality must be done with care, however, because natural deviations from the well-defined $^{204}Pb/^{203}Tl$ ratio of CCs (1.43 ± 0.14, 2SD; Baker et al. 2010) are expected for ECs and particularly OCs (e.g., Fig. 1). Parnallee, in particular, is characterized by near-primordial Pb with $^{206}Pb/^{204}Pb = 11.85$ and a fairly high $^{204}Pb/^{203}Tl$ ratio of 28.1 (Table 1).

The recent ^{205}Pb-^{205}Tl isochron studies of CCs (Baker et al. 2010) and iron meteorites (Nielsen et al. 2006a; Andreasen et al. 2012) also encountered problems with terrestrial Pb contamination but were able to apply relatively simple mass balance calculations to quantify and correct for such effects. While such calculations are imprecise, particularly at high levels of contamination due to the unknown isotope composition of the extraneous Pb, they are relatively straightforward because CCs and iron meteorites are characterized by very low μ and are hence expected to have primordial or near-primordial indigenous Pb isotope compositions. Due to the presence of radiogenic Pb in our ECs and OCs, a more sophisticated approach must be employed to estimate the isotope composition and mass fraction of indigenous meteoritic Pb in the samples. Such calculations were carried out here using an approach that is explained and discussed in the supporting information. Briefly, the U and Th contents of the samples were first estimated (as they were not measured in this study) and subsequently employed to infer in situ ingrowth of radiogenic Pb. The final estimates for the molar fraction of indigenous meteoritic Pb present in meteorites ($f_{met\text{-}Pb}$) were then obtained with a solver, which minimized the difference between measured Pb isotope composition of a sample and the calculated mixture (of primordial Pb + radiogenic Pb + terrestrial Pb), using the known (measured) total Pb concentration as an additional constraint (see supporting information for details). The results of these calculations ($f_{met\text{-}Pb}$; Table 1) take into account uncertainties in the estimated U, Th concentrations of the samples and the isotope composition of the terrestrial contaminant. The quoted uncertainties for $f_{met\text{-}Pb}$ (Table 1) are deemed to be reasonable for meteorites where U, Th contents are provided in the literature but they may be larger for samples where such data were not available and mean U, Th concentrations estimated for ECs and OCs were used instead. While all $f_{met\text{-}Pb}$ values of Table 1 are model-based estimates, the results for the latter samples must be assessed with particular care and they are thus given in parentheses.

Taking the calculated $f_{met\text{-}Pb}$ values at face value, the data reveal that the extent of Pb contamination is highly variable for the analyzed meteorites, ranging from nearly 0% to almost 100%, whereby modern terrestrial Pb provides more than 50% of the present-day Pb content for 15 of 29 samples (Table 1). The calculated extent of contamination is thereby in good agreement with qualitative assessments based on the $^{204}Pb/^{203}Tl$ ratios (Fig. 2b). In detail, the calculations confirm that the most contaminated samples are Indarch and Atlanta among the ECs ($f_{met\text{-}Pb} \leq 0.2$) and Ausson, New Concord, and Marion (Iowa) among L chondrites ($f_{met\text{-}Pb} < 0.15$). For the LL chondrites, the $f_{met\text{-}Pb}$ estimates confirm that Benares, Khanpur, Appley Bridge, and Dhurmsala contain not only minor indigenous meteoritic Pb (at <30%) but also reveal similarly severe Pb contamination for other meteorites (Bishunpur, Tuxtuac, Mangwendi) with only Parnallee characterized by $f_{met\text{-}Pb} > 75\%$ (Table 1).

Pb-Pb Isochrons

All isochrons were evaluated in "inverse" $^{207}Pb/^{206}Pb$ versus $^{204}Pb/^{206}$ Pb isotope space (Table 2), with ages determined using the Isoplot Visual Basic "add-in" (v3.41b) of Ludwig (2003) for Microsoft Excel.

Enstatite Chondrites

When all ECs are considered, a $^{207}Pb/^{206}Pb$ age of 4497 + 85 Ma is obtained, while exclusion of two clearly contaminated samples (Indarch, Atlanta) yields a much more precise result of 4553 ± 18 Ma (Table 2). The latter age is thereby in good agreement with a Pb-Pb isochron age of 4577 ± 8 Ma obtained by Manhes and Allègre (1978) for the ECs Indarch EH4, Saint Saveur EH5, Saint Mark's EH5, and Hvittis

Table 2. Pb-Pb ages for the enstatite and ordinary chondrites.

Chondrite class/group	Samples	*n*	Age (Ma)	±2SD (Ma)
Enstatite chondrites	All	8	4497	85
Enstatite chondrites	Excluding Atlanta, Indarch	6	4553	18
EH chondrites	Excluding Indarch[a]	2	4527	1
EL chondrites	Excluding Atlanta	4	4559	6
L chondrites	All	10	4533	77
L chondrites	Excluding Ausson, New Concord, Marion	7	4543	87
L chondrites	Excluding Ausson, Alfianello, New Concord, Barwell, Marion	6	4535	37
LL chondrites	All	10	4519	100
LL chondrites	Excluding Benares, Appley Bridge, Dhurmsala	7	4542	170
LL chondrites	Excluding Benares, Khanpur, Tuxtuac, Appley Bridge, Dhurmsala	5	4568	280

Regression calculated with Isoplot v3.41b using the "Model 2" fit, which assigns equal weights and zero error correlations to each point (Ludwig 2003). "Inverse" Pb-Pb ages derived using present-day $^{238}U/^{235}U = 137.88$, and decay constants of $\lambda^{235}U = 0.98571\ Ga^{-1}$ (Mattinson 2010) and $\lambda^{238}U = 0.155125\ Ga^{-1}$ (Jaffey et al. 1971).

[a]The low age uncertainty reflects that this is a two-point isochron.

EL6. However, although early investigations suggested a common parent body for EH and EL chondrites (e.g., Kaczaral et al. 1988; Kong et al. 1997), a number of petrographic, elemental, and isotopic studies now indicate that these two groups are derived from separate parent bodies (e.g., Sears et al. 1982; Keil 1989; Lin and Goresy 2002; Savage and Moynier 2013), and individual isochrons are hence discussed in the following.

Following elimination of strongly contaminated Indarch (Table 1), the remaining EH chondrites Abee and St Marks yield a two-point isochron with an age of 4527 Ma. This is clearly younger than the concordant Pb-Pb age of 4582 ± 6 Ma quoted for St Marks (Manhes and Allègre 1978) and the ^{53}Mn-^{53}Cr isochron ages of ~4565 Ma determined for the EH4 chondrites Abee and Indarch (Shukolyukov and Lugmair 2004), which are thought to reflect parent–daughter fractionation during condensation in the solar nebula. The relatively young age obtained here is thereby likely an artifact of the significant terrestrial Pb contamination recorded for our sample of St Marks (Table 1; $f_{met\text{-}Pb} \approx$ 24–58%).

For the EL chondrites, the samples remaining after exclusion of Atlanta ($f_{met\text{-}Pb} \leq 19\%$; Table 1) have relatively pristine Pb isotope compositions, although a detailed evaluation of contamination was not possible for NWA 3134 (see supporting information). Notably, these samples define the most precise and meaningful Pb-Pb isochron of this study, equivalent to an age of 4559 ± 6 Ma. This result is identical, within error, to the less precise Pb-Pb age of 4588 ± 28 Ma for Hvittis EL6 (Manhes and Allègre 1978) and the ~4560 Ma ^{53}Mn-^{53}Cr age for Khairpur EL6, which are thought to record metamorphic equilibration on the parent body (Shukolyukov and Lugmair 2004).

Ordinary Chondrites

Using the data for all L chondrites, the $^{207}Pb/^{206}Pb$ isochron age is 4533 ± 77 Ma. When three (Ausson, New Concord, and Marion) or five (plus Alfianello and Barwell) samples with the most obvious terrestrial Pb contamination are excluded, similar ages of 4543 ± 87 Ma and 4535 ± 37 Ma, respectively, are obtained (Table 2). Given the uncertainties, these results agree with published Pb-Pb ages of between 4529 and 4553 Ma for three L5/L6 chondrites (Manhes and Allègre 1978), of ~4550 Ma for L4/L5/L6 chondrites (Unruh 1982), and of about 4525–4555 Ma for silicates and phosphates of L5/L6 chondrites (Göpel et al. 1994; Bouvier et al. 2007), which together are thought to reflect the protracted metamorphic history of the parent body.

For the LL chondrites, the complete data set yields a $^{207}Pb/^{206}Pb$ isochron age of 4519 ± 100 Ma. Exclusion of three (Benares, Appley Bridge, and Dhurmsala) or five (plus Khanpur and Tuxtuac) of the most contaminated samples that all have Pb isotope compositions resembling terrestrial Pb produces even less precise isochron ages of 4542 ± 170 Ma and 4568 ± 280 Ma, respectively (Table 2). While these results are consistent with published Pb-Pb ages of about 4545–4557 Ma for silicates and phosphates of LL5/LL6 chondrites (Manhes et al. 1978; Göpel et al. 1994; Bouvier et al. 2007), which are considered to record metamorphic equilibration and cooling, the agreement is unsurprising given the large uncertainties of our LL chondrite ages.

In summary, the new Pb-Pb ages for OCs are only of limited utility due to the large associated errors. This reflects that precise Pb-Pb dating was not a key aim of this investigation such that no attempts were made to separate and analyze phases with particularly radiogenic Pb isotope compositions (e.g., phosphates and

leachates) or remove terrestrial Pb through initial leaching of the samples. As a consequence, even the most pristine OCs analyzed here feature a significant component of terrestrial Pb (Table 1), which overprints the metamorphic cooling history of the samples.

Cd and Tl Isotope Compositions—Evaluation of Stable Isotope Fractionation

Application of the ^{205}Pb-^{205}Tl decay system for chronometry is rendered difficult if radiogenic variations in Tl isotope compositions are overlain by stable isotope effects. Such fractionations are evaluated in the following, in particular based on the stable Cd isotope data that were acquired here for ECs (Fig. 3) and are published in the literature for OCs (Wombacher et al. 2003, 2008). For comparison, the Cd isotope compositions of the CCs analyzed by Baker et al. (2010) are also shown in Fig. 3. Notably, most of the latter chondrites (seven of nine samples) show a restricted range of $\varepsilon^{114/110}$Cd between +1.1 and +5.3. The higher $\varepsilon^{114/110}$Cd values of the two anomalous samples, Kainsaz CO3 (+15.6) and Leoville CV3 (+32.7), were previously interpreted to reflect stable isotope fractionation that occurred during elemental mobilization associated with heating and metamorphism on the parent body (Wombacher et al. 2008; Baker et al. 2010).

Enstatite Chondrites

The $\varepsilon^{114/110}$Cd data for the ECs are highly variable with most meteorites (six of eight samples) showing results between +2.9 and +10.4 and two samples (Khairpur EL6; PCA 91020 EL3) with extremely fractionated values of +65.7 and +72.9 (Fig. 3). Overall, the ECs thus display more variable Cd isotope compositions than CCs, which indicate that many samples record significant stable isotope fractionation, most likely as a result of parent body processes. The impact of such processes on Tl isotope compositions is also apparent. In detail, seven of the eight ECs for which isotopic data are available (excluding Khairpur EL6) define a strong linear correlation between ε^{205}Tl and $\varepsilon^{114/110}$Cd but the near-perfect correlation (R^2 = 0.99) is largely governed by a single sample, PCA 91020 (Fig. 3a). However, the correlation is still significant (with R^2 = 0.60) if only the six samples with the least fractionated Cd isotope compositions are considered (Fig. 3b). In addition, the elemental data reveal an excellent correlation between Cd and Tl abundances for the ECs (Fig. 1a), a trend that is also broadly linked to petrological type, whereby higher concentrations are generally observed in less equilibrated meteorites.

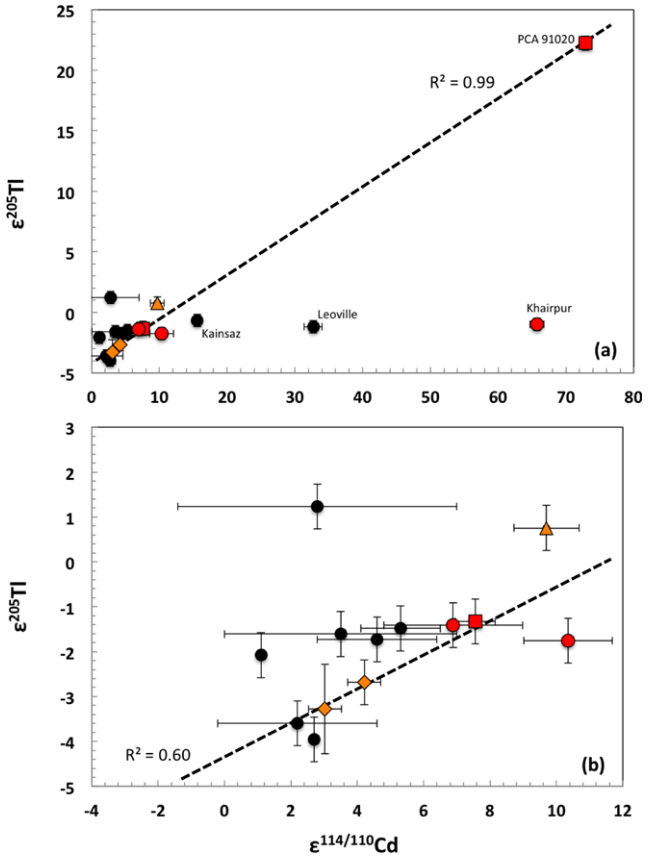

Fig. 3. Plots of ε^{205}Tl versus $\varepsilon^{114/110}$Cd for the enstatite chondrites of this study and the carbonaceous chondrites analyzed by Baker et al. (2010). Variable scaling is applied in panels (a) and (b) to best reveal the systematics of the results. The hashed lines denote the best-fit correlation (and correlation coefficient) for all samples except Khairpur (panel a) and except Khairpur and PCA 91020 (panel b). Symbols are as defined in the legend of Fig. 1. (Color figure can be viewed at wileyonlinelibrary.com.)

Together, the observations suggest that the abundances and isotope compositions of Cd and Tl are significantly controlled by the degree to which they were remobilized on the parent bodies. Additional constraints emerge when the data are scrutinized in more detail. In particular, PCA 91020 (EL3) and Abee (EH4) are more enriched in Cd but more depleted in Tl than MAC 02839 (EL3) and Indarch (EH4), respectively (Table 1). It is conceivable that these systematics reflect the distinct behavior of Cd and Tl during thermal metamorphism and mobilization, as has been observed in thermally altered CCs and heating experiments with carbonaceous material (e.g., Matza and Lipschutz 1977; Ngo and Lipschutz 1980; Paul and Lipschutz 1989; Wombacher et al. 2008; Tonui et al. 2014). It may also indicate that processes other than thermal metamorphism affected the Cd and Tl contents of these meteorites. Notably, Abee,

with shock grades S2 to S4, shows brecciation from multiple impact events (Rubin and Scott 1997). Elemental mobilization at the high temperatures associated with shock processing may have altered the volatile budgets of this meteorite, although it displays nearly unfractionated isotope compositions ($\varepsilon^{114/110}$Cd = +3.0; ε^{205}Tl = −3.3; Table 1). Such isotope fractionation, however, is evident for the most heavily shocked EC analyzed in this study, PCA 91020 with a shock stage of S5 (Rubin et al. 1997). The finding that this meteorite has the heaviest Tl and Cd isotope compositions recorded in this study (ε^{205}Tl = +22.2; $\varepsilon^{114/110}$Cd = +72.9) suggests that stable isotope fractionation is likely associated with the heating and elemental volatilization that occurs during impacts. Similarly, shock effects may also be present in other meteorites, such as Khairpur (EL6, S2; $\varepsilon^{114/110}$Cd = +65.7) and Atlanta (EL6, S2; $\varepsilon^{114/110}$Cd = +10.4), even though they nominally record lower shock stages. In this case, the meteorites were possibly highly shocked prior to metamorphism but the petrological shock features were subsequently erased by thermal annealing (Rubin 1983; Rubin et al. 1997). Given these uncertainties, it is problematic to unambiguously assign the mobilization and stable isotope fractionation observed for Cd and Tl in ECs to *either* thermal or shock metamorphism, with both processes likely contributing to the volatile element signatures of most samples.

Ordinary Chondrites

While no stable Cd isotope analyses were carried out for OCs, abundant data for such meteorites are available in the literature (Wombacher et al. 2003, 2008). Notably, the studies of Wombacher and coworkers demonstrate highly variable Cd isotope compositions for OCs, with $\varepsilon^{114/110}$Cd values ranging from about −110 to +150. A similar isotopic variability was observed for H, L, and LL chondrites and particularly large isotope effects were seen for type 3 OCs. These findings were interpreted in the context of an "onion layer" parent body model for the OCs, as reflecting widespread redistribution and associated isotope fractionation of Cd during numerous episodes of partial evaporation and condensation during thermal metamorphism. However, it was also suggested that elemental redistribution and isotope fractionation was possibly enhanced by impact-induced breakup and reassembly of meteorite parent bodies (Friedrich et al. 2004; Wombacher et al. 2008).

These observations are in accord with the data of the present study. Notably, our samples show highly variable Tl isotope compositions that are unlikely to solely reflect differences in radiogenic ingrowth of ^{205}Tl at variable Pb/Tl ratios (Fig. 4; see Discussion section).

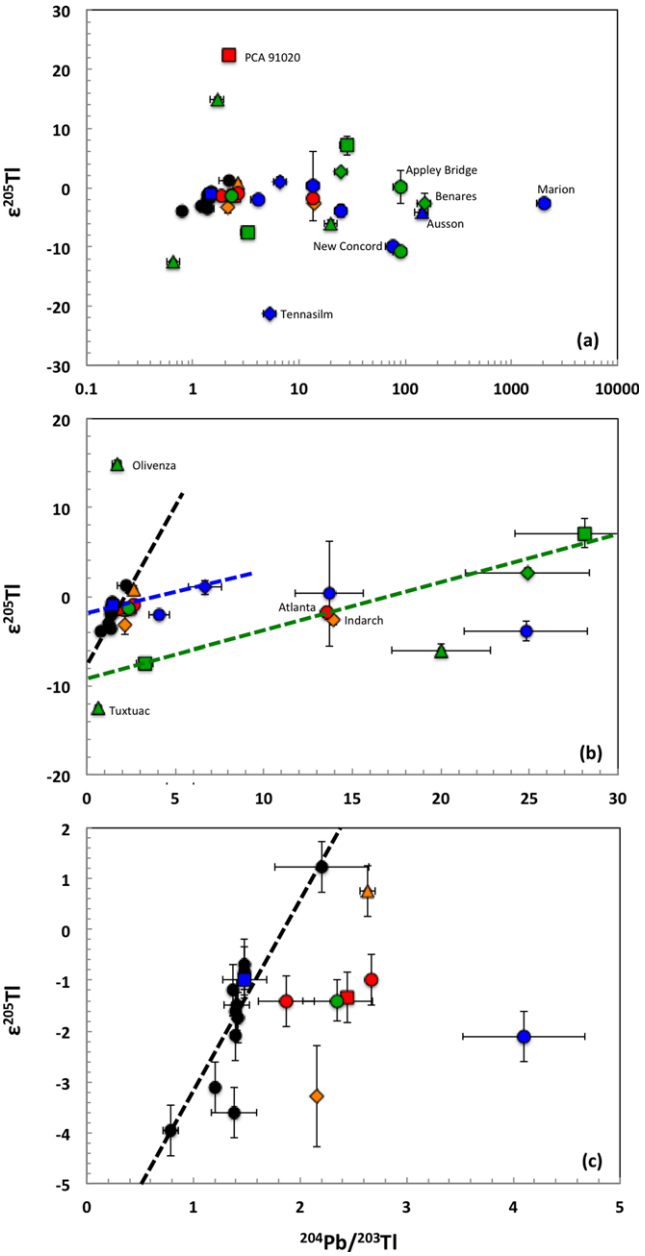

Fig. 4. Plots of ε^{205}Tl versus measured ^{204}Pb/^{203}Tl ratios for the enstatite and ordinary chondrites of this study as well as the carbonaceous chondrites analyzed by Baker et al. (2010). Variable scaling is used in panels (a) to (c) to best reveal the structure and systematics of the data. The blue and green hashed lines in panel (b) highlight correlations for particularly pristine samples that are discussed in the text as possible ^{205}Pb-^{205}Tl isochrons for L and LL chondrites, respectively. The hashed black lines in panels (b) and (c) denote the ^{205}Pb-^{205}Tl isochron of carbonaceous chondrites determined by Baker et al. (2010). Symbols are as defined in the legend of Fig. 1. (Color figure can be viewed at wileyonlinelibrary.com.)

Furthermore, most equilibrated L6/LL6 chondrites record a very narrow range of ε^{205}Tl values from −3.9 to +0.3 and, with only few exceptions (particularly

among LL chondrites), the OCs are in accord with higher Tl and Cd concentrations for lower petrographic grades. Together, these results attest to significant stable isotope fractionation of both Cd and Tl during the elemental remobilization that accompanies parent body metamorphism. Additional isotope fractionation during shock metamorphism is also possible but is likely to have played a secondary role. This interpretation follows from the observation that most OCs analyzed in this study record only minor shock (S2, S3), even though there are a few notable exceptions, such as New Concord (S4) and Alfianello (S5) (Table 1). Furthermore, the data set reveals no clear correlations between Tl concentrations or isotope composition and shock grade, in accord with the Cd isotope findings of Wombacher et al. (2008) for OCs.

Tl Isotope Compositions and $^{204}Pb/^{203}Tl$—Evidence for Live ^{205}Pb

In comparison to the CCs, the ECs and particularly the OCs display significantly larger variations in Tl isotope compositions and $^{204}Pb/^{203}Tl$ ratios (Fig. 4). Despite this large variability, evidence for the former existence of live ^{205}Pb is not straightforward to find, as both Tl isotope fractionation and Pb contamination obscure the effects of ^{205}Tl ingrowth from the decay of ^{205}Pb.

Enstatite Chondrites

For ECs, the Tl isotope compositions of all but one sample show variability similar to that seen in the CCs, with $\varepsilon^{205}Tl$ values between −3.0 and +0.8, while the anomalous sample PCA 91020 extends this range to $\varepsilon^{205}Tl = +22.2$ (Fig. 4a). For $^{204}Pb/^{203}Tl$, most samples fall within a narrow range of between about 1.9 and 2.7, but one from each group (Indarch EH4 and Atlanta EL6) has $^{204}Pb/^{203}Tl \approx 14$ (Fig. 4b). In addition, Daniel's Kuil is characterized by $^{204}Pb/^{203}Tl \approx 42$ but this sample is not plotted in Figs. 3 and 4 because isotopic data are not available.

The high $^{204}Pb/^{203}Tl$ ratios of Indarch (EH4) and Atlanta (EL6) are almost certainly a product of terrestrial Pb contamination (with $f_{met\text{-}Pb}$ <20%; Table 1) and the data are hence unsuitable for isochron calculations. Similarly, the high and hence possibly radiogenic $\varepsilon^{205}Tl = +22.2$ for PCA 91020 is accompanied by an extremely fractionated Cd isotope composition, suggestive of stable isotope fractionation (Figs. 3a and 4). The remaining five ECs display a far more restricted range of Tl isotope compositions and $^{204}Pb/^{203}Tl$ ratios, which might be interpreted to define a correlation that is offset from, but nearly subparallel to, the data array of the CCs (Fig. 4c). Interpretation of this correlation as an isochron is unlikely to be robust, however, given the significant Cd isotope fractionations and the correlated Cd and Tl isotope compositions observed for the ECs (Fig. 3).

In summary, these findings indicate that the $\varepsilon^{205}Tl$ values of ECs may well show some variability that reflects in situ decay of ^{205}Pb but this cannot be convincingly separated from the stable isotope effects, which are likely to have also impacted Tl isotope compositions. A detailed evaluation of possible radiogenic variations of $\varepsilon^{205}Tl$ is furthermore complicated by the terrestrial Pb contamination, which significantly perturbs the $^{204}Pb/^{203}Tl$ ratios of many ECs (Table 1).

L Chondrites

For the L chondrites, $\varepsilon^{205}Tl$ varies between −21.3, the lowest value measured for this isotope system to date, and +1.0, while $^{204}Pb/^{203}Tl$ ranges from a CC-like value of 1.5 for Mezö-Madaras L3.7 up to a highly anomalous ratio of 2030 for Marion (Fig. 4). The latter result and the high $^{204}Pb/^{203}Tl$ ratios of Ausson ($^{204}Pb/^{203}Tl = 144$), New Concord ($^{204}Pb/^{203}Tl = 76$), and Barwell ($^{204}Pb/^{203}Tl = 25$) are likely an artifact of terrestrial Pb contamination with $f_{met\text{-}Pb}$ estimates of <15% for all meteorites but Barwell ($f_{met\text{-}Pb}$ = 20–40%; Table 1).

Mezö-Madaras resembles a CC, both in terms of $^{204}Pb/^{203}Tl$ ratio and $\varepsilon^{205}Tl$ (Fig. 4c), in agreement with its highly volatile-rich composition and unequilibrated petrology, which indicates only weak thermal processing. In contrast, the most anomalous Tl isotope compositions are seen for Tennasilm L4 ($\varepsilon^{205}Tl \approx -21$) and New Concord L6 ($\varepsilon^{205}Tl \approx -10$), even though these meteorites have very different Tl concentrations of about 4.8 ng g^{-1} and 0.35 ng g^{-1}, respectively. Given that large Cd stable isotope fractionations were documented for L chondrites (Wombacher et al. 2008), it is likely that the Tl isotope compositions of Tennasilm and New Concord were also altered by stable isotope effects and this cannot be ruled out for other L chondrites.

When considering only those samples which are least likely to be perturbed by terrestrial Pb contamination (with $f_{met\text{-}Pb} > 0.4$) and Tl stable isotope fractionation ($\varepsilon^{205}Tl \geq -10$), the L chondrites show limited evidence of live ^{205}Pb. Focusing on the two most weakly metamorphosed and pristine meteorites, Mezö-Madaras L3.7 and Saratov L4, these define a two-point isochron that provides an initial $^{205}Pb/^{204}Pb = (9.1 \pm 4.1) \times 10^{-5}$ (Fig. 4b, blue dashed line), equivalent to a Pb-Tl age of 65 + 17/−25 Ma (or 39–82 Ma) for L3/L4 chondrites relative to CCs. Given the evidence for significant addition of terrestrial Pb to

Table 3. Data for ^{205}Pb-^{205}Tl isochron calculations that apply meteoritic ^{204}Pb/^{203}Tl ratios corrected for terrestrial Pb contamination.

	$f_{met\text{-}Pb}$[a]	^{204}Pb/^{203}Ti meteoritic [b]	±[b]	ε^{205}Tl[c]	±2SD[c]
L chondrite isochron					
Mezo-Madaras	0.76–0.88	1.29	0.26	−1.0	0.3
Saratov	0.38–0.91	4.1	3.0	1.0	0.8
Mocs 54647	0.43–0.92	7.3	7.1	0.3	5.9
LL chondrite isochron					
Bishunpur	0.18–0.37	1.2	0.6	−7.5	0.5
Parnallee	≥0.82	26.1	6.0	7.1	1.6
Soko-Banja	0.53–0.72	17.5	4.7	2.7	0.5

[a]Estimated molar fraction of indigenous meteoritic Pb in the meteorite samples. Data from Table 1 obtained using calculations outlined in the supporting information.
[b]Estimated indigenous meteoritic ^{204}Pb/^{203}Tl ratios of the samples, following correction for terrestrial Pb contamination as outlined in the supporting information. The uncertainties incorporate both measurement errors and the uncertainty in $f_{met\text{-}Pb}$.
[c]Data from Table 1.

these and other L chondrites (Table 1), it is more useful to investigate possible isochron relationships using ^{204}Pb/^{203}Tl data that are corrected for such contamination (Table 3; see supporting information). In this case, the two-point isochron of Mezö-Madaras and Saratov defines an initial ^{205}Pb/^{204}Pb of $(1.7 \pm 1.9) \times 10^{-4}$. This suggests equilibration of the Pb-Tl system more than 22 Ma after CCs, but is also in accord with the absence of any live ^{205}Pb on the parent body (Fig. 5, blue dashed line). A similar but slightly more precise result emerges when Mocs 54647 is also considered in the isochron calculation. This equilibrated L6 chondrite displays radiogenic Pb (^{206}Pb/^{204}Pb ≈ 39; Table 1), which is indicative of only limited Pb contamination ($f_{met\text{-}Pb}$ = 43–92%) and possibly a very low primordial Pb content (Table 3). An L chondrite isochron defined by Mezö-Madaras, Saratov, and Mocs 54647 also yields a highly uncertain initial ^{205}Pb/^{204}Pb = $(1.5 \pm 1.4) \times 10^{-4}$, which is in accord with late equilibration of the Pb-Tl system at 54 + 60/−28 Ma, equivalent to 26–113 Ma after CCs (Fig. 5, solid blue line).

LL Chondrites

Among the chondrites studied to date, the LL group displays the largest range of Tl isotope compositions, with ε^{205}Tl values of between −12.5 and +14.9. The ^{204}Pb/^{203}Tl ratios are also highly variable, with results ranging from 0.66 to 152 (Fig. 4). Notably, the three samples with the highest ^{204}Pb/^{203}Tl of between 90 and 152 (Benares LL4; Appley Bridge, Dhurmsala both LL6) have ^{206}Pb/^{204}Pb of between about 17.4 and 19.4, while Khanpur LL5 and Tuxtuac

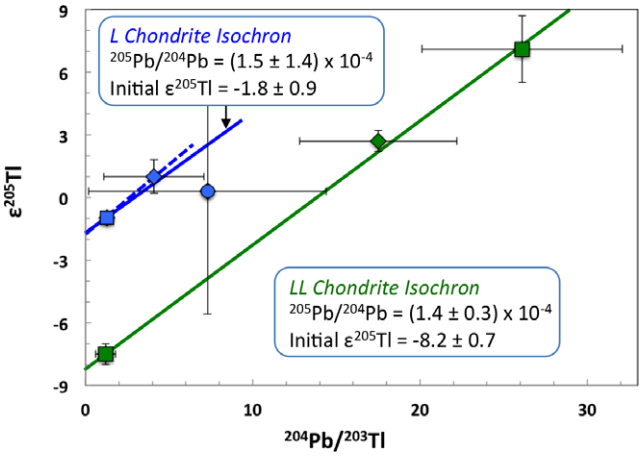

Fig. 5. Isochron plot of ε^{205}Tl versus ^{204}Pb/^{203}Tl for particularly pristine L chondrites (in blue) and LL chondrites (in green), as summarized in Table 3. In contrast to Fig. 4, the ^{204}Pb/^{203}Tl ratios plotted here are corrected for terrestrial Pb contamination. The ^{205}Pb-^{205}Tl isochrons defined by the three L and LL chondrites are shown as solid lines, while the dashed blue line denotes the correlation defined by the L3/L4 chondrites Mezö-Madaras and Saratov (see text for details). Symbols are as defined in the legend of Fig. 1. (Color figure can be viewed at wileyonlinelibrary.com.)

LL5 feature Pb isotope compositions akin to terrestrial surface environments with ^{206}Pb/^{204}Pb of 18.1 and 18.8, respectively (Table 1). These characteristics are indicative of significant terrestrial Pb contamination with $f_{met\text{-}Pb} \leq 30\%$, such that the indigenous meteoritic ^{204}Pb/^{203}Tl ratios of the samples cannot be constrained precisely.

Further results for the two samples with the most extreme Tl isotope compositions, Tuxtuac (ε^{205}Tl ≈ −12) and Olivenza (ε^{205}Tl ≈ +15), also give rise to suspicion. Notably, both meteorites are heavily metamorphosed LL5 chondrites. Tuxtuac has a low Pb concentration and a ^{204}Pb/^{203}Tl ratio that is lower than found in any CC (Figs. 1b and 4b). As it also has a terrestrial Pb isotope composition, the Pb content of this meteorite most likely reflects exchange with terrestrial Pb and overall Pb loss. In contrast, Olivenza features a much higher Pb concentration coupled with relatively high Tl, which produces a ^{204}Pb/^{203}Tl similar to that of CCs. In addition, it has a relatively low ^{206}Pb/^{204}Pb ≈ 13.2, indicative of a fairly uncontaminated Pb budget with $f_{met\text{-}Pb}$ = 50–68% (Table 1). However, given the comparatively low Pb/Tl ratio and ε^{205}Tl = +14.9, Olivenza plots far above the ^{205}Pb-^{205}Tl isochron of CCs, regardless of the exact slope of the latter (Fig. 4b). For this positive ε^{205}Tl to be of radiogenic origin, Olivenza would need to be derived from a parent body that was originally characterized by very high Pb/Tl, followed by significant Pb loss, either on the parent asteroid or by the meteoroid. While

possible, such an evolution is considered less likely than a scenario whereby the high ε^{205}Tl is due to stable isotope fractionation.

Consideration of only the least metamorphosed (LL3 and LL4) and least contaminated (Table 1) samples, Bishunpur LL3.1, Parnallee LL3.6, and Soko-Banja LL4, hints at a correlation between ε^{205}Tl and ^{204}Pb/^{203}Tl (Fig. 4b, dashed green line). If interpreted as an isochron, this correlation defines an initial ^{205}Pb/^{204}Pb of $(1.26 \pm 0.17) \times 10^{-4}$, equivalent to an age of 58 + 11/−24 Ma (34–69 Ma) relative to CCs. Given that the Pb budgets of these meteorites are subject to significant terrestrial contamination (Table 1), it is again more useful to evaluate possible isochronous relationships using ^{204}Pb/^{203}Tl data corrected for terrestrial Pb contamination. Such a correction yields lower ^{204}Pb/^{203}Tl ratios for all meteorites but the change is particularly prominent for Soko-Banja, with ^{204}Pb/^{203}Tl decreasing from ~25 to ~18 (Table 3). Notably, the contamination-corrected ^{204}Pb/^{203}Tl data also provide a precisely defined correlation (Fig. 5, green line). This is unlikely to be a fortuitous outcome, given the clear evidence for terrestrial Pb contamination of the samples, but suggests that the correction procedure produces robust results.

Evaluation of the revised isochron yields an initial ^{205}Pb/^{204}Pb ratio of $(1.4 \pm 0.3) \times 10^{-4}$, equivalent to an age of 55 + 12/−24 Ma (31–67 Ma) for LL3/LL4 chondrites after CCs. Notably, this result is remarkably similar to the isochron age obtained using the uncorrected ^{204}Pb/^{203}Tl ratios. Overall, the data thus provide credible evidence for the former presence of live ^{205}Pb on the LL chondrite parent body during cooling. The youngest possible ^{205}Pb-^{205}Tl age of 31 Ma after CCs is thereby still younger than the Pb-Pb ages of about 4545–4557 Ma, which were determined for silicates and phosphates of LL5/LL6 chondrites (Manhes et al. 1978; Göpel et al. 1994; Bouvier et al. 2007), and that are thought to record the cooling history of the parent body. This observation suggests a low closure temperature for the ^{205}Pb-^{205}Tl system relative to U-Pb closure in silicates (at ~1000–1100 K; Cherniak 2001) and phosphates (~800 K; Cherniak et al. 1991), in accord with the highly mobile character of Tl even during moderate thermal overprinting (Matza and Lipschutz 1977; Ngo and Lipschutz 1980).

CONCLUSIONS

Thallium, Pb, and Cd concentration and Tl, Pb isotope analyses were carried out for enstatite as well as L- and LL-type ordinary chondrites, with additional Cd isotope measurements for the former. The Tl and Cd contents of all three suites typically vary by 1–2 orders of magnitude and for the enstatite and L chondrites, the concentrations are well correlated with petrographic grade, whereby less metamorphosed samples have the highest abundances of both elements. This feature was most likely established during parent body metamorphism and associated mobilization of volatile elements. The Pb contents reveal less variability and Pb isotope compositions suggest that this reflects pervasive contamination of many meteorites with terrestrial Pb. Model calculations indicate that more than 50% of the total measured Pb concentrations for 15 of 29 samples are due to addition of modern Pb. In part, this accounts for the relatively young and imprecise Pb-Pb ages determined for EH, L, and LL chondrites, which are of little chronological utility. In contrast, four relatively pristine EL chondrites with $f_{met\text{-}Pb} > 80\%$ define a precise Pb-Pb age of 4559 ± 6 Ma, in accord with the metamorphic cooling ages determined for equilibrated EL chondrites in previous studies (Manhes and Allègre 1978; Shukolyukov and Lugmair 2004).

The Cd isotope compositions of the ECs are variable due to stable isotope fractionation, whereby two samples have $\varepsilon^{114/110}$Cd ≈ +70 and the remainder display $\varepsilon^{114/110}$Cd values of about +3 to +10. All but one of these meteorites is characterized by ε^{205}Tl of between −3.3 and +0.8, while PCA 910020 features ε^{205}Tl ≈ +22, presumably due to coupled fractionation of both Cd and Tl stable isotopes. Excluding PCA 910020 and three meteorites with ^{204}Pb/^{203}Tl >14 (due to Pb contamination), the remaining five ECs might be interpreted to define a ^{205}Pb-^{205}Tl isochron. This interpretation is questionable, however, as a correlation of ε^{205}Tl with $\varepsilon^{114/110}$Cd is supported by all but one of these samples. This covariation suggests that at least some of the observed Tl isotope variability reflects stable isotope fractionation rather than radiogenic ingrowth from decay of ^{205}Pb. The available evidence, including the shock history of the meteorites, thereby suggests that the observed Cd and Tl stable isotope effects are a consequence of elemental mobilization during both thermal and shock metamorphism on the parent body.

The ε^{205}Tl data for most L chondrites range between −4 and +1 but there are two outliers with ε^{205}Tl ≤ −10, which probably reflect stable isotope effects associated with elemental remobilization during metamorphism. Evaluation of the samples that show the least evidence for Pb contamination or stable Tl isotope fractionation provides an initial ^{205}Pb/^{204}Pb of $(1.5 \pm 1.4) \times 10^{-4}$, in accord with late equilibration of the ^{205}Pb-^{205}Tl system at 26–113 Ma after CCs.

The LL chondrites display highly variable ^{204}Pb/^{203}Tl ratios and the most variable Tl isotope compositions seen in this study, with ε^{205}Tl between

−12.5 and +14.9. Data evaluation suggests that the highest $^{204}Pb/^{203}Tl$ ratios are due to Pb contamination, while the most extreme Tl isotope compositions reflect stable isotope fractionation. Persuasive evidence for in situ decay of ^{205}Pb is, however, provided by three particularly pristine samples, all LL3/LL4 chondrites, which display an excellent correlation between $\varepsilon^{205}Tl$ and $^{204}Pb/^{203}Tl$. Interpretation of this correlation as an isochron yields an initial $^{205}Pb/^{204}Pb = (1.4 \pm 0.3) \times 10^{-4}$, equivalent to a metamorphic cooling age of 31–67 Ma for LL3/LL4 chondrites relative to CCs.

In summary, our analyses reveal highly variable indigenous Tl and Cd contents in ECs and OCs, while the Pb concentrations are strongly affected by terrestrial contamination. In addition, the Tl isotope compositions of some but possibly many meteorites were altered by stable isotope fractionation. Together, these issues hinder the search for evidence of live ^{205}Pb in both ECs and OCs, and restrict the chronological application of the ^{205}Pb-^{205}Tl decay system. However, with more basic understanding, the sensitivity with which Tl and Cd concentrations and isotope compositions react to secondary mobilization and alteration processes might be exploited to improve understanding of both nebular and parent body processes that affect volatile element budgets and distributions.

Acknowledgments—The MAGIC group is thanked for help in keeping the mass spec running and the clean laboratories organized. We are grateful to the Natural History Museum in London for providing the great majority of meteorites used in this study. The reviewers Sune Nielsen and Frank Wombacher as well as Associate Editor Gopalan Srinivasan are thanked for their careful and constructive reviews, which were instrumental in crafting an improved version of the manuscript. This research was supported by STFC research grants to MR (ST/J001260/1, ST/N000803/1) as well as MR and MS (ST/F002157/1), an STFC studentship to CP, a Janet Watson studentship of the Department of Earth Science & Engineering to AS, and a Fellowship of the Danish Research Council to RA.

Editorial Handling—Dr. Gopalan Srinivasan

REFERENCES

Abouchami W., Galer S. J. G., Horner T. J., Rehkämper M., Wombacher F., Xue Z., Lambelet M., Gault-Ringold M., Stirling C. H., Schönbächler M., Shiel A. E., Weis D., and Holdship P. F. 2013. A common reference material for cadmium isotope studies—NIST SRM 3108. *Geostandards and Geoanalytical Research* 37:5–17.

Amelin Y. 2006. The prospect of high-precision Pb isotopic dating of meteorites. *Meteoritics & Planetary Science* 41:7–17.

Anders E. and Stevens C. M. 1960. Search for extinct lead 205 in meteorites. *Journal of Geophysical Research* 65:3043–3047.

Andreasen R., Rehkämper M., Benedix G. K., Theis K. J., Schönbächler M., and Smith C. L. 2012. Lead-thallium chronology of IIAB and IIIAB iron meteorites and the solar system initial abundance of lead-205 (abstract #2902). 43rd Lunar and Planetary Science Conference. CD-ROM.

Arden J. W. 1983. Distribution of lead and thallium in the matrix of the Allende meteorite and the extent of terrestrial lead contamination in chondrites. *Earth and Planetary Science Letters* 62:395–406.

Baker R. G. A., Rehkämper M., Hinkley T. K., Nielsen S. G., and Toutain J. P. 2009. Investigation of thallium fluxes from subaerial volcanism—Implications for the present and past mass balance of thallium in the oceans. *Geochimica et Cosmochimica Acta* 73:6340–6359.

Baker R. G. A., Schönbächler M., Rehkämper M., Williams H., and Halliday A. N. 2010. The thallium isotope composition of carbonaceous chondrites—New evidence for live ^{205}Pb in the early solar system. *Earth and Planetary Science Letters* 291:39–47.

Bennett M. E. and McSween H. Y. 1996. Shock features in iron-nickel metal and troilite of L-group ordinary chondrites. *Meteoritics & Planetary Science* 31:255–264.

Blake J. B., Lee T., and Schramm D. N. 1973. Chronometer for s-process nucleosynthesis. *Nature Physical Science* 242:98–101.

Bouvier A., Blichert-Toft J., Moynier F., Vervoort J. D., and Albarede F. 2007. Pb-Pb dating constraints on the accretion and cooling history of chondrites. *Geochimica et Cosmochimica Acta* 71:1583–1604.

Chen J. H. and Wasserburg G. J. 1994. The abundance of thallium and primordial lead in selected meteorites—The search for ^{205}Pb. Proceedings, 25th Lunar and Planetary Science Conference. pp. 245–246.

Cherniak D. J. 2001. Pb diffusion in Cr diopside, augite, and enstatite, and consideration of the dependence of cation diffusion in pyroxene on oxygen fugacity. *Chemical Geology* 177:381–397.

Cherniak D. J., Lanford W. A., and Ryerson F. J. 1991. Lead diffusion in apatite and zircon using ion implantation and Rutherford Backscattering techniques. *Geochimica et Cosmochimica Acta* 55:1663–1673.

Connolly H. C., Smith C., Benedix G., Folco L., Righter K., Zipfel J., Yamaguchi A., and Aoudjehane H. C. 2007. The Meteoritical Bulletin, No. 92. *Meteoritics & Planetary Science* 42:1647–1694.

Friedrich J. M., Bridges J. C., Wang M.-S., and Lipschutz M. E. 2004. Chemical studies of L chondrites. VI: Variations with petrographic type and shock-loading among equilibrated falls. *Geochimica et Cosmochimica Acta* 68:2889–2904.

Galer S. J. G. and Abouchami W. 1998. Practical application of lead triple spiking for the correction of instrumental mass discrimination. *Mineral Magazine* 62A:491–492.

Gattacceca J., Rochette P., Denise M., Consolmagno G., and Folco L. 2005. An impact origin for the foliation of chondrites. *Earth and Planetary Science Letters* 234:351–368.

Göpel C., Manhès G., and Allègre C. J. 1985. U-Pb systematics in iron meteorites: Uniformity of primordial lead. *Geochimica et Cosmochimica Acta* 49:1681–1695.

Göpel C., Manhès G., and Allègre C. J. 1994. U-Pb systematics of phosphates from equilibrated ordinary chondrites. *Earth and Planetary Science Letters* 121:153–171.

Hettmann K., Marks M. A. W., Kreissig K., Zack T., Wenzel T., Rehkämper M., Jacob D. E., and Markl G. 2014. The geochemistry of Tl and its isotopes during magmatic and hydrothermal processes: The peralkaline Ilimaussaq complex, southwest Greenland. *Chemical Geology* 366:1–13.

Heymann D. and Liffman K. 1986. Isotopic compositions of bismuth, lead, thallium and mercury from mini r-processing. *Meteoritics* 21:95–108.

Huey J. M. and Kohman T. P. 1972. Search for extinct natural radioactivity of ^{205}Pb via thallium-isotope anomalies in chondrites and lunar soil. *Earth and Planetary Science Letters* 16:401–412.

Izawa M. R. M., Flemming R. L., Banerjee N. R., and McCausland P. J. A. 2011. Micro-X-ray diffraction assessment of shock stage in enstatite chondrites. *Meteoritics & Planetary Science* 46:638–651.

Jaffey A. H., Flynn K. F., Glendenin L. E., Bentley W. C., and Essling A. M. 1971. Precision measurement of half-lives and specific activities of ^{235}U and ^{238}U. *Physical Review C* 4:1889–1906.

Jochum K. P., Nohl U., Herwig K., Lammel E., Stoll B., and Hofmann A. W. 2005. GeoReM: A new geochemical database for reference materials and isotopic standards. *Geostandards and Geoanalytical Research* 29:333–338.

Kaczaral P. W., Dennison J. E., Verkouteren R. M., and Lipschutz M. E. 1988. On volatile/mobile trace element trends in E3 chondrites. *Proceedings of the NIPR Symposium on Antarctic Meteorites* 12:113–121.

Keil K. 1989. Enstatite meteorites and their parent bodies. *Meteoritics* 24:195–208.

Kong P., Mori T., and Ebihara M. 1997. Compositional continuity of enstatite chondrites and implications for heterogeneous accretion of the enstatite chondrite parent body. *Geochimica et Cosmochimica Acta* 61:4895–4914.

Lin Y. and Goresy A. E. 2002. A comparative study of opaque phases in Qingzhen (EH3) and MacAlpine Hills 88136 (EL3): Representatives of EH and EL parent bodies. *Meteoritics & Planetary Science* 37:577–599.

Lodders K. 2003. Solar system abundances and condensation temperatures of the elements. *The Astrophysical Journal* 591:1220–1247.

Ludwig K. 2003. *Isoplot 3.00—A geochronological toolkit for Microsoft Excel*. Berkeley, California: Berkeley Geochronology Center. 71 p.

Manhes G. and Allègre C. J. 1978. Time differences as determined from the ratio of lead 207 to lead 206 in concordant meteorites. *Meteoritics* 13:543–548.

Manhes G., Minster J. F., and Allègre C. J. 1978. Comparative uranium-thorium-lead and rubidium-strontium study of the Saint Sèverin amphoterite: Consequences for early solar system chronology. *Earth and Planetary Science Letters* 39:14–24.

Mattinson J. M. 2010. Analysis of the relative decay constants of ^{235}U and ^{238}U by multi-step CA-TIMS measurements of closed-system natural zircon samples. *Chemical Geology* 275:186–198.

Matza S. D. and Lipschutz M. E. 1977. Thermal metamorphism of primitive meteorites—VI. Eleven trace elements in Murchison C2 chondrite heated at 400–1000°C. Proceedings, 8th Lunar Science Conference. pp. 161–176.

Ngo H. T. and Lipschutz M. E. 1980. Thermal metamorphism of primitive meteorites—X. Additional trace elements in Allende (C3V) heated to 1400°C. *Geochimica et Cosmochimica Acta* 44:731–739.

Nielsen S. G. and Rehkämper M. 2012. Thallium isotopes and their application to problems in earth and environmental science. In *Handbook of environmental isotope geochemistry: Advances in isotope geochemistry, part 2*, edited by Baskaran M. Berlin: Springer. pp. 247–269.

Nielsen S. G., Rehkämper M., Baker J., and Halliday A. N. 2004. The precise and accurate determination of thallium isotope compositions and concentrations for water samples by MC-ICPMS. *Chemical Geology* 204:109–124.

Nielsen S. G., Rehkämper M., and Halliday A. N. 2006a. Thallium isotopic variations in iron meteorites and evidence for live lead-205 in the early solar system. *Geochimica et Cosmochimica Acta* 70:2643–2657.

Nielsen S. G., Rehkämper M., Teagle D. A. H., Butterfield D. A., Alt J. C., and Halliday A. N. 2006b. Hydrothermal fluid fluxes calculated from the isotopic mass balance of thallium in the ocean crust. *Earth and Planetary Science Letters* 251:120–133.

Nielsen S. G., Rehkämper M., Norman M. D., Halliday A. N., and Harrison D. 2006c. Thallium isotopic evidence for ferromanganese sediments in the mantle source of Hawaiian basalts. *Nature* 439:314–317.

Nielsen S. G., Wasylenki L. E., Rehkämper M., Peacock C. L., Xue Z., and Moon E. M. 2013. Towards an understanding of thallium isotope fractionation during adsorption to manganese oxides. *Geochimica et Cosmochimica Acta* 117:252–265.

Nielsen S. G., Rehkämper M., and Prytulak J. 2017. Investigation and application of thallium isotope fractionation. In *Measurements, theories and applications of non-traditional stable isotopes*, edited by Teng F.-Z., Watkins J., and Dauphas N. Washington, D.C.: Mineralogical Society of America. pp. 759–798.

Ostic R. G., El-Badry H. M., and Kohmann T. P. 1969. Isotopic composition of meteoritic thallium. *Earth and Planetary Science Letters* 7:72–76.

Palme H. and Jones A. 2005. Solar system abundances of the elements. In *Meteorites, comets and planets*, edited by Davis A. M. Amsterdam: Elsevier. pp. 41–61.

Paul R. L. and Lipschutz M. E. 1989. Labile trace elements in some Antarctic carbonaceous chondrites: Antarctic and non-Antarctic meteorite comparisons. *Zeitschrift für Naturforschung* 44a:979–987.

Pengra J. G., Genz H., and Fink R. W. 1978. Orbital electron capture ratios in the decay of ^{205}Pb. *Nuclear Physics A* 302:1–11.

Prytulak J., Nielsen S. G., Plank T., Barker M., and Elliott T. 2013. Assessing the utility of thallium and thallium isotopes for tracing subduction zone inputs to the Mariana arc. *Chemical Geology* 345:139–149.

Rehkämper M. and Halliday A. N. 1999. The precise measurement of Tl isotopic compositions by MC-ICPMS: Application to the analysis of geological materials and meteorites. *Geochimica et Cosmochimica Acta* 63:935–944.

Rehkämper M. and Mezger K. 2000. Investigation of matrix effects for Pb isotope ratio measurements by multiple collector ICP-MS: Verification and application of optimized analytical protocols. *Journal of Analytical Atomic Spectrometry* 15:1451–1460.

Rehkämper M., Frank M., Hein J. R., Porcelli D., Halliday A. N., Ingri J., and Liebetrau V. 2002. Thallium isotope variations in seawater and hydrogenetic, diagenetic, and hydrothermal ferromanganese deposits. *Earth and Planetary Science Letters* 197:65–81.

Rehkämper M., Wombacher F., Horner T. J., and Xue Z. 2011. Natural and anthropogenic cadmium isotope variations. In *Handbook of environmental isotope geochemistry*, edited by Baskaran M. Berlin: Springer. pp. 125–154.

Righter K. and Satterwhite C. 2004. *Antarctic Meteorite Newsletter February 2004*. Houston, Texas: NASA Johnson Space Center.

Ripperger S. and Rehkämper M. 2007. Precise determination of cadmium isotope fractionation in seawater by double-spike MC-ICPMS. *Geochimica et Cosmochimica Acta* 71:631–642.

Rubin A. E. 1983. The Atlanta enstatite chondrite breccia. *Meteoritics* 18:113–121.

Rubin A. E. 1994. Metallic copper in ordinary chondrites. *Meteoritics* 29:93–98.

Rubin A. E. 2004. Postshock annealing and postannealing shock in equilibrated ordinary chondrites: Implications for the thermal and shock histories of chondritic asteroids. *Geochimica et Cosmochimica Acta* 68:673–689.

Rubin A. E. and Scott E. R. D. 1997. Abee and related EH chondrite impact-melt breccias. *Geochimica et Cosmochimica Acta* 61:425–435.

Rubin A. E., Scott E. R. D., and Keil K. 1997. Shock metamorphism of enstatite chondrites. *Geochimica et Cosmochimica Acta* 61:847–858.

Savage P. S. and Moynier F. 2013. Silicon isotopic variation in enstatite meteorites: Clues to their origin and Earth-forming material. *Earth and Planetary Science Letters* 361:487–496.

Schauble E. A. 2007. Role of nuclear volume in driving equilibrium stable isotope fractionation of mercury, thallium, and other very heavy elements. *Geochimica et Cosmochimica Acta* 71:2170–2189.

Sears D. W., Kallemeyn G. W., and Wasson J. T. 1982. The compositional classification of chondrites: II The enstatite chondrite groups. *Geochimica et Cosmochimica Acta* 46:597–608.

Shukolyukov A. and Lugmair G. W. 2004. Manganese-chromium isotope systematics of enstatite meteorites. *Geochimica et Cosmochimica Acta* 68:2875–2888.

Stöffler D., Keil K., and Edward R. D. S. 1991. Shock metamorphism of ordinary chondrites. *Geochimica et Cosmochimica Acta* 55:3845–3867.

Tera F. and Carlson R. W. 1999. Assessment of the Pb–Pb and U-Pb chronometry of the early solar system. *Geochimica et Cosmochimica Acta* 63:1877–1889.

Tonui E., Zolensky M., Hiroi T., Nakamura T., Lipschutz M. E., Wang M.-S., and Okudaira K. 2014. Petrographic, chemical and spectroscopic evidence for thermal metamorphism in carbonaceous chondrites I: CI and CM chondrites. *Geochimica et Cosmochimica Acta* 126:284–306.

Unruh D. M. 1982. The U-Th-Pb age of equilibrated L chondrites and a solution to the excess radiogenic Pb problem in chondrites. *Earth and Planetary Science Letters* 58:75–94.

Wasserburg G. J., Busso M., Gallino R., and Raiteri C. M. 1994. Asymptotic giant branch stars as a source of short-lived radioactive nuclei in the solar nebula. *The Astrophysical Journal* 424:412–428.

Wasserburg G. J., Busso M., Gallino R., and Nollet K. M. 2006. Short-lived nuclei in the early solar system: Possible AGB sources. *Nuclear Physics A* 777:5–69.

Wiggenhauser M., Bigalke M., Imseng M., Müller M., Keller A., Murphy K., Kreissig K., Rehkämper M., Wilcke W., and Frossard E. 2016. Cadmium isotope fractionation in soil-wheat systems. *Environmental Science and Technology* 50:9223–9231.

Wombacher F., Rehkämper M., Mezger K., and Münker C. 2003. Stable isotope compositions of cadmium in geological materials and meteorites determined by multiple collector-ICPMS. *Geochimica et Cosmochimica Acta* 67:4639–4654.

Wombacher F., Rehkämper M., Mezger K., and Münker C. 2004. Determination of the mass-dependence of cadmium isotope fractionation during evaporation. *Geochimica et Cosmochimica Acta* 68:2349–2357.

Wombacher F., Rehkämper M., Mezger K., Bischoff A., and Münker C. 2008. Cadmium stable isotope cosmochemistry. *Geochimica et Cosmochimica Acta* 72:646–667.

Xue Z., Rehkämper M., Schönbächler M., Statham P. J., and Coles B. J. 2012. A new methodology for precise cadmium isotope analyses of seawater. *Analytical and Bioanalytical Chemistry* 402:883–893.

Yokoi K., Takahashi K., and Arnould M. 1985. The production and survival of ^{205}Pb in stars and the ^{205}Pb-^{205}Tl s-process chronometry. *Astronomy & Astrophysics* 145:339–346.

APPENDIX

Table A1. Cd concentrations of the carbonaceous chondrites analyzed by Baker et al. (2010).

Sample	Group	Cd (ng g^{-1})	±Cd (ng g^{-1})
Orgueil	CI1	669	13
Cold Bokkeveld	CM2	350	7
Murchison	CM2	387	8
Leoville	CV3	36.9	0.7
Allende (Smithsonian)	CV3	231	5
NWA 801	CR2	95.4	1.9

Cd concentrations are only available for samples to which the Cd double spike was added before the separation chemistry.

SUPPORTING INFORMATION

Additional supporting information may be found in the online version of this article:

Fig. S1. Flowchart of the full analytical procedure for the determination of Cd-Tl-Pb concentrations and isotope compositions.

Table S1. Anion exchange chemistry for the separation of Pb and Tl from spiked sample solution aliquots for subsequent concentration measurements by isotope dilution MC-ICP-MS.

Table S2. Anion exchange chemistry for the separation of Cd from spiked sample solution aliquots, for subsequent Cd concentration measurements by isotope dilution MC-ICP-MS.

Table S3. Anion exchange chemistry for the separation of a combined Pb-Cd and a Tl fraction from sample solutions for subsequent measurements of isotope compositions.

Table S4. Anion exchange chemistry for purification of Tl fractions obtained from the first-stage chemistry of Table S3.

Table S5. Anion exchange chemistry for the separation and purification of Pb and Cd from the combined Pb-Cd fractions obtained from the first-stage chemistry of Table S3.

Table S6. Chromatographic procedure for purification of Cd from the Cd fractions obtained from the second-stage chemistry of Table S5.

Table S7. Published U-Th concentration data determined by mass spectrometry for samples relevant to this study.

Table S8. Estimated mass fractions of meteoritic Pb in the samples ($f_{met\text{-}Pb}$) and key parameters that constrain the estimates. Presentation and discussion of modeling to estimate terrestrial Pb contamination of meteorites.